Components Irradiation Test 15

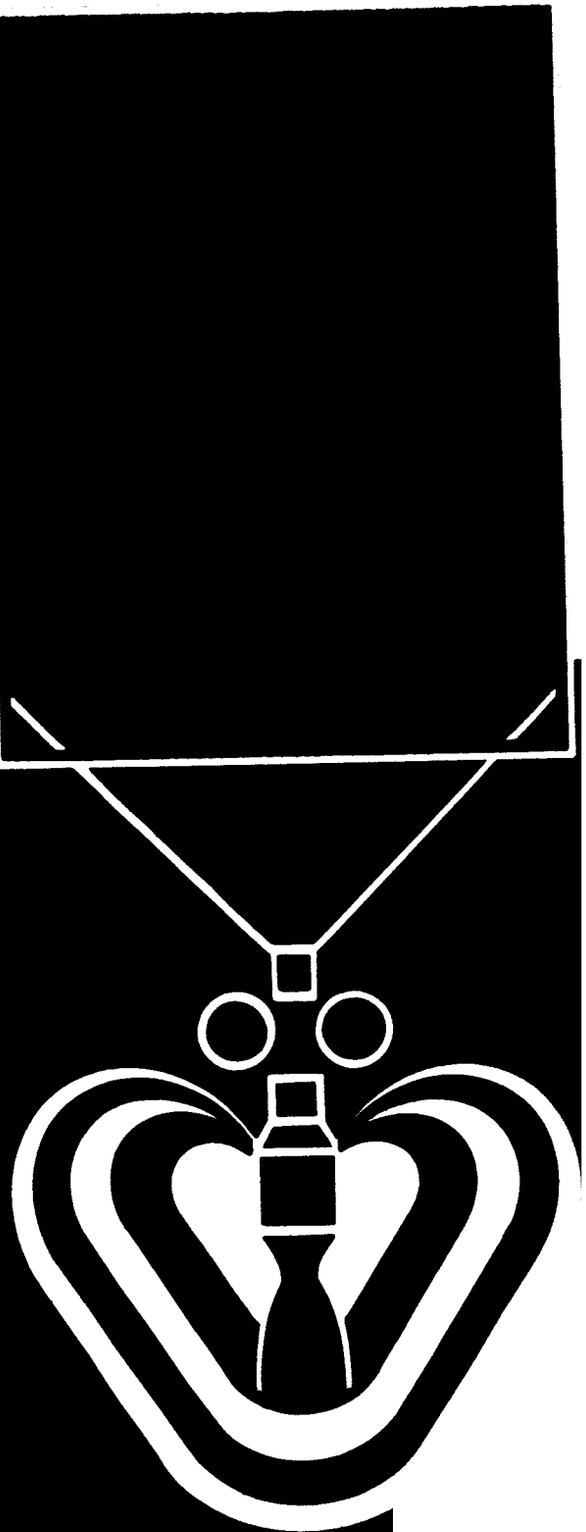

Georgia Nuclear Laboratories

LOCKHEED-GEORGIA COMPANY -- A Division of Lockheed Aircraft Corporation

ER 8006

COMPONENTS IRRADIATION TEST NO. 15
2N708, 2N918, S2N1486 AND
S2N2412 TRANSISTORS AND
2N2498 FIELD EFFECT TRANSISTOR

June 1965

Prepared For:

GEORGE C. MARSHALL SPACE FLIGHT CENTER

Prepared By:

GEORGIA NUCLEAR LABORATORIES

GEORGIA NUCLEAR LABORATORIES
Lockheed-Georgia Company - A Division of Lockheed Aircraft Corporation

If this document is supplied under the requirements of a United States Government contract, the following legend shall apply unless the letter U appears in the coding box.

This data is furnished under a United States Government contract and only those portions hereof which are marked (for example, by circling, underscoring or otherwise) and indicated as being subject to this legend shall not be released outside the Government (except to foreign governments, subject to these same limitations), nor be disclosed, used, or duplicated, for procurement or manufacturing purposes, except as otherwise authorized by contract, without the permission of Lockheed-Georgia Company, A Division of Lockheed Aircraft Corporation, Marietta, Georgia. This legend shall be marked on any reproduction hereon in whole or in part.

The "otherwise marking" and "indicated portions" as used above shall mean this statement and include all details or manufacture contained herein respectively.

Code U	Contract NAS 8-5332

FOREWORD

This report is submitted to the Astrionics Laboratory of the George C. Marshall Space Flight Center, National Aeronautics and Space Administration, Huntsville, Alabama, in accordance with the requirements of Task Order No. ASTR-LGC-26 of Contract No. NAS 8-5332. The report is one of a series describing radiation effects on various electronic components. This particular report concerns four types of transistors, and one type of field effect transistor. The tests were performed by the Georgia Nuclear Laboratories, Dawsonville, Georgia.

TABLE OF CONTENTS

LIST OF TABLES AND FIGURES

LIST OF TABLES AND FIGURES
(Continued)

LIST OF TABLES AND FIGURES
(Continued)

LIST OF TABLES AND FIGURES
(Continued)

Page

Figures

1.0 SUMMARY

Four types of injection type transistors and one type of field effect transistor were subjected to a radiation environment. Measurements were made to determine the effect of the radiation on the h_{FE} and h_{ie} parameters of the injection type transistors and on the I_{DSS}, V_P, g_{m_o} and g_{m_1} parameters of the field effect transistor.

The specimens tested were:

Number	Type	Manufacturer	Tested at (°C)
20	2N708	Fairchild	75
20	2N708	Fairchild	30
20	2N918	Fairchild	75
20	2N918	Fairchild	30
10	S2N1486	Silicon Transistor Corporation	30
20	S2N2412	Texas Instruments	30
29	2N2498	Texas Instruments	30

The test data indicated:

For the injection type transistors

(1) All specimens failed (50% decrease in h_{FE}). Ranges of failures were:

Type	First Failure	Last Failure
2N708(75°C)	4.1×10^{13} n/cm^2	8.8×10^{13} n/cm^2
2N708(30°C)	2.2×10^{13} n/cm^2	7.3×10^{13} n/cm^2
2N918(75°C)	7.9×10^{13} n/cm^2	5.3×10^{14} n/cm^2
2N918(30°C)	3.5×10^{13} n/cm^2	1.8×10^{14} n/cm^2
S2N1486	2.4×10^{10} n/cm^2	5.9×10^{10} n/cm^2
S2N2412	1.6×10^{13} n/cm^2	2.8×10^{13} n/cm^2

(2) Normalized h_{ie} decreased in a manner very similar to normalized h_{FE}.

For the 2N2498 field effect transistor

(1) I_{DSS} remained essentially constant up to an exposure of 1×10^{13} n/cm^2 then began to decrease, reaching essentially zero at 1.7×10^{15} n/cm^2.

(2) V_p showed a radiation rate effect at a reactor power of 3 megawatts. The net effect of the radiation exposure was about a 70% decrease in V_p.

(3) Both g_{m_o} and g_{m_j} decreased as a result of the irradiation.

(4) All specimens failed (50% decrease in g_{m_o}). Failures ranged from 3.0×10^{14} n/cm^2 to 7.4×10^{14} n/cm^2.

2.0 INTRODUCTION

The experiment described in this report is the fifteenth irradiation of electronic components and is the nineteenth in a series of radiation effects tests on electronic equipment, circuits, and components contemplated for use on a nuclear space vehicle. Since the use of equipment on this vehicle is contingent upon its ability to withstand the nuclear environment, the Astrionics Laboratory of the Marshall Space Flight Center has undertaken to assure that Government furnished or specified equipment will survive this environment. The equipment is to be subjected to the expected nuclear environment as simulated at the Georgia Nuclear Laboratories. Measurements made on the equipment during the irradiation will describe its radiation tolerance.

The subjects of this test are the types 2N708, 2N918, S2N1486 and S2N2412 transistors and the type 2N2498 field effect transistor.

3.0 TEST PROCEDURE

The test specimens were supplied by the Astrionics Laboratory of the Marshall Space Flight Center. Throughout the test, 20 of the 2N708 transistors and 20 of the 2N918 transistors were mounted in a controlled temperature chamber adjusted to hold the temperature at 75 ± 2°C. All the other specimens were mounted in a controlled temperature chamber adjusted to hold the temperature at 30 ± 2°C. The specimens were first exposed to a nominal gamma dose of 6.3×10^5 r behind a neutron attenuator shield. The shielding was then removed and the test was continued until a nominal integrated neutron flux of 2.6×10^{14} n/cm^2 was accumulated. At this point the reactor was shut down for a period of about 15 hours. The reactor was then restarted and the irradiation was continued until a nominal integrated neutron flux of 1.8×10^{15} n/cm^2 had been accumulated. The total nominal gamma dose at the end of the test was 1.3×10^7 r. Before, during and after the irradiation, measurements were made on non-failed specimens to determine the parameters listed in Table 1. Measurements were also made during the test to define the nuclear and temperature environments.

3.1 TEST SPECIMENS

The specimens tested are listed in Table 1. Except for the S2N1486 devices the specimens tested were mounted on printed circuit boards by the Astrionics Laboratory. The S2N1486 devices were mounted by GNL. All specimens were new units and had only been subjected to MSFC receiving inspection. Manufacturers' specifications for the specimens are shown in Table 2. The specimen boards were mounted vertically in the radiation field to equalize the radiation flux distribution. Figures 1, 2, 3 and 4 show the relative positions of the specimens. The environmental chambers in which the specimens were placed were located directly adjacent to the reactor for the irradiation.

3.2 TEST SPECIMEN MEASUREMENTS

A complete set of data was taken prior to reactor start-up to establish baseline data for the test. During the irradiation, measurements were made at all reactor power settings. Measurements were also made:

(a) during reactor shutdown for removal of the shield,
(b) at the beginning and the end of the 15 hour reactor shutdown period,
(c) upon completion of the irradiation, and
(d) approximately 66 hours after the end of the irradiation.

The measurements were made on all non-failed specimens and were performed with the test fixture in place at the reactor facility.

3.3 INSTRUMENTATION

3.3.1 Injection Type Transistor Measurement Circuits

The measurement circuits for the injection type transistors are shown in Figures 5, 6 and 7. The emitters of the test specimens were commoned, and the base and collector were commutated into the test circuits.

In the h_{ie} and h_{FE} measurement circuits the feedback loop, including Amplifier A, establishes the base current necessary to provide the collector current shown in Table 1. Capacitors of 910 picofarads were connected from collector to emitter of the 2N708, 2N918 and the S2N2412 specimens on the printed circuit board to prevent oscillation caused by the inductance and capacitance of the long instrumentation cables. These were mica capacitors which had previously shown tolerance in excess of the radiation levels experienced in this test. The base current was measured by the digital voltmeter and h_{FE} was calculated from these measurements.

With a signal as shown in Figures 5, 6 and 7 applied to the base, the base to emitter voltage (V_{be}) was measured by an AC voltmeter. These values were used in the determination of input impedance (h_{ie}).

3.3.2 Field Effect Transistor Measurement Circuits

Figures 8 and 9 show the circuits for measuring transconductance under two different sets of test conditions. The circuit in Figure 8 was also used to monitor I_D and V_{GS}, and the circuit in Figure 9 was also used to measure I_{DSS}. The circuit shown in Figure 10 was used to measure V_p (pinch-off voltage).

3.4 TEST ENVIRONMENT

3.4.1 Pressure

During the test all specimens were at atmospheric pressure.

3.4.2 Temperature

Twenty 2N708 and twenty 2N918 transistor specimens were located in an environmental chamber at a temperature of 75 ± 2°C throughout the test. The remaining specimens were located in an environmental chamber adjusted to hold the temperature at 30 ± 2°C. Near the end of the test the temperature in this chamber increased because of gamma heating. See Figures 11 and 12 for the temperature traces for the specimens located in the 30°C chamber.

3.4.3 Nuclear

The irradiation was performed in two radiation phases with a lapse of about one hour between phases. The first phase was conducted using neutron attenuation shielding interposed between the reactor and the specimens. The second phase was

without shielding. This latter phase was interrupted by a period of about 15 hours at zero reactor power. The neutron to gamma ratio was 2.6×10^5 nvt/r with shielding and 1.5×10^8 nvt/r after shielding had been removed. During the irradiation both neutron and gamma radiations were monitored and recorded.* Isoline radiation flux plots were made for use in data reduction.

A more detailed description of the GNL Nuclear Measurement System is contained in a previous report, viz; Components Irradiation Test No. 1, ER-6785, Georgia Nuclear Laboratories, Dawsonville, Georgia.

4.0 METHOD OF DATA ANALYSIS

The GNL Data Logging System recorded the parameter measurements in type-written digital form and simultaneously punched the data in five-channel perforated tape. A tape-to-card converter was used to transfer the data to IBM cards which were then programmed into an IBM 7094 computer to yield the parameters portrayed in the included graphs.

Normalization of a parameter was accomplished by dividing each parameter value by its corresponding pre-irradiation value.

The mean parameter value for a data group, where shown, was computed by adding the individual specimen parameter values and dividing the sum by the number of specimens.

The median parameter value for a data group (that value which divides a distribution so that an equal number of items is on either side of it) was determined from a plot of the individual specimen parameter values on an arithmetic probability chart. The limits of the 68% envelopes were determined by picking off those values within which were contained 34% of the specimens next above the group median value and 34% of the specimens next below the group median value. The limits of the 95% envelopes were found in a similar fashion. The 7094 computer performed these functions.

In those cases where the parameter of an individual specimen behaved significantly differently from the group median, these "unusual" specimens have been portrayed separately.

The 2N2498 specimens were located on two boards, numbers 7 and 8 (Figure 4). Because the reactor had to be positioned higher than usual to accommodate the greater

vertical extent of the test arrangement, the flux field over these boards was such that the variation in radiation exposure for individual specimens ranged from 27% to 101% of the nominal exposure. This wide variation precluded treating all 29 specimens as a single group for statistical analysis. However, in order to obtain some statistical intelligence from the data, the 29 specimens were divided into three groups. One group contained 14 specimens with accumulated neutron fluxes ranging from 80% to 101% of the nominal, a second group contained 8 specimens with accumulated neutron fluxes from 59% to 77%, and the last group had 7 specimens with accumulated fluxes from 27% to 47%. Mean parameter values were calculated for each group and these means were plotted at the respective group average integrated neutron fluxes. The maximum and minimum parameter values were also plotted. These plotted points were used to delineate the means and envelopes shown in the figures portraying the 2N2498 data. The envelopes correspond approximately to the 95% envelopes shown in other figures of this report. The post-test values shown in these figures are those obtained from the 14 specimen group as this was the group experiencing the maximum integrated neutron flux.

Radiation environmental data shown in the figures' abscissae were obtained by integrating, with respect to time, the gamma dose rates and neutron fluxes. Those figures which show "Percent Failed Versus Integrated Neutron Flux" were prepared in a manner similar to the procedure described by Mr. Frank W. Poblenz in an article entitled "Analysis of Transistor Failure in a Nuclear Environment", which appeared in Volume NS-10, Number 1, January 1963, of the IEEE Transactions on Nuclear Science. This type of presentation enables the circuit designer to predict with 50% confidence the radiation level at which any given percentage of the particular component will equal or exceed the failure criteria.

Copies of the reduced data from which the graphs were prepared are on file in the Astrionics Laboratory of the George C. Marshall Space Flight Center, NASA, Huntsville, Alabama, and the Georgia Nuclear Laboratories, Lockheed-Georgia Company, Dawsonville, Georgia.

5.0 TEST DATA AND DISCUSSION OF RESULTS

The test data have been presented herein in graphical form. The radiation exposure is, in all cases, a combination of neutrons and gamma rays. The abscissa scale on each of the graphs is accumulated neutrons/cm^2 greater than 0.5 MeV. However, the coincident accumulated gamma dose (r) is also indicated at those points where changes in the reactor power rate occurred. It is important to remember that the total radiation exposure consists of both neutrons and gamma rays and that each may contribute, in varying degrees, to the degradation of a component's parameter.

5.1 TYPE 2N708 TRANSISTOR

Twenty specimens were irradiated at a constant 75 ± 2°C. Twenty additional specimens were irradiated in a chamber adjusted to 30 ± 2°C; however, gamma heating during the latter part of the test caused the temperature in the chamber to rise above the specified limits. Temperature data for these specimens are shown in Figure 11.

5.1.1 2N708 Specimens Irradiated at 75°C

The h_{FE} Parameter

Figure 13 shows the normalized h_{FE} data for these specimens. The slope discontinuity in the median at the point of shield removal indicates that the gamma component of the irradiation contributed significantly to the degradation in h_{FE}. One specimen displayed a significant increase in h_{FE} during the first part of the irradiation. This specimen is shown in Figure 14. The post-test measurements taken about 66 hours after the end of the test indicated no annealing of the h_{FE} parameter.

Figure 15 shows the failure (50% decrease in h_{FE}) pattern for the group. Initial

values of h_{FE} and order of failure were:

h_{FE_o}	Order of Failure
37.36	15
38.14	5
42.13	19
42.40	10
43.03	8
43.03	3
44.99	17
45.64	14
46.06	13
47.24	20
49.75	11
50.84	6
51.50	2
52.44	1
52.72	16
54.06	18
54.34	4
55.24	12
63.78	7
65.07	9

These data show a slight correlation between high values of h_{FE_o} and early failure.

The h_{ie} Parameter

The normalized h_{ie} data are shown in Figure 16. The general similarity of these data to the normalized h_{FE} data shown in Figure 13 may be explained by the

relationship:

$$h_{ie} = r_b + (h_{fe} + 1)r_e$$

where r_b = base spreading resistance, and
r_e = emitter junction resistance.

Since $h_{fe} \approx h_{FE}$ the expression may be written:

$$h_{ie} \approx r_b + (h_{FE} + 1)r_e \ .$$

Normally $(h_{FE} + 1)r_e$ is the predominant factor and thus controls h_{ie}.

The fact that normalized h_{ie} (Figure 16) decreased at a rate different from normalized h_{FE} (Figure 13) indicates that either r_b or r_e, or both, may have been changed by the irradiation.

There appeared to be a slight annealing of h_{ie} during periods of zero reactor rate.

5.1.2 2N708 Specimens Irradiated at 30°C

The h_{FE} Parameter

The normalized h_{FE} data for these specimens are shown in Figures 17 and 18. These data also show a discontinuity in the slope of the median at the point of shield removal indicating a significant contribution by the gamma irradiation to the degradation of h_{FE}.

The failure (50% decrease in h_{FE}) pattern for the group is shown in Figure 19. A comparison of Figures 15 and 19 shows no significant difference between the failure

pattern of those specimens irradiated at 75°C and that of those specimens irradiated at 30°C.

Initial values of h_{FE} and order of failure were:

h_{FE_o}	Order of Failure
31.05	14
31.08	11
31.79	17
33.32	15
34.00	7
36.32	12
36.51	19
38.46	8
38.70	10
39.20	9
39.84	2
41.50	3
42.20	18
42.36	20
45.25	6
46.67	1
47.15	5
50.33	16
51.01	13
54.00	4

The data also show a slight correlation between high value of h_{FE_o} and early failure.

The h_{ie} Parameter

The normalized h_{ie} data are shown in Figure 20. The remarks of paragraph 5.1.1 concerning the h_{ie} Parameter apply to the general similarity of Figures 17 and 20.

These specimens, in contrast to those at 75°C, showed no significant annealing of h_{ie} during periods of zero radiation.

5.2 TYPE 2N918 TRANSISTOR

Twenty specimens were irradiated at a constant 75 ± 2°C. Twenty additional specimens were irradiated in a chamber adjusted to 30 ± 2°C; however, gamma heating during the latter part of the test caused the temperature in the chamber to rise above the specified limits. Temperature data for these specimens are shown in Figure 11.

5.2.1 2N918 Specimens Irradiated at 75°C

The h_{FE} Parameter

The h_{FE} data for these specimens are presented in Figures 21 and 22. The contribution of the gamma component of the irradiation to the degradation of h_{FE} is evidenced by the slope discontinuity of the median at the point of shield removal. This discontinuity is not very pronounced in the case of the "unusual" specimen (Figure 22), and may indicate that this specimen was more gamma-resistant than were the other specimens. This may explain why this specimen was the last in the group to fail.

Figure 23 shows the failure pattern for these specimens. Initial values of h_{FE} and order of failure were:

h_{FE_o}	Order of Failure
10.78	19
34.72	17
34.83	15
37.55	11
37.87	16
39.20	10
41.40	6
42.00	9
42.18	8
42.91	14
43.27	5
46.19	12
49.36	4
51.27	1
57.47	13
61.16	2
62.39	3
62.47	18
100.90	7

(The data obtained from one specimen were not useable.)

These data show fairly good correlation between high values of h_{FE_o} and early failure.

The h_{ie} Parameter

Figure 24 shows the normalized h_{ie} data for these specimens. The discussion in

paragraph 5.1.1 concerning the h_{ie} Parameter applies to the general similarities between Figures 21 and 24.

There appeared to be a slight annealing of h_{ie} during periods of no irradiation.

5.2.2 2N918 Specimens Irradiated at 30°C

The h_{FE} Parameter

The normalized h_{FE} data for these specimens are shown in Figure 25. The characteristic slope discontinuity in the median at the point of shield removal also appears in this figure.

Figure 26 shows the failure pattern for the group. A comparison of Figures 23 and 26 shows that the group irradiated at 75°C (Figure 23) had slightly greater radiation tolerance than did the 30°C group. Initial values of h_{FE} and order of failure were:

h_{FE_o}	Order of Failure
22.41	15
26.13	14
28.81	16
29.56	20
30.93	18
34.01	12
34.58	17
34.71	9
37.87	8
38.40	5

h_{FE_o}	Order of Failure (Continued)
39.43	13
40.89	10
41.32	19
43.96	4
47.37	7
52.08	11
52.08	3
52.88	1
53.17	2
53.36	6

These data show good correlation between high values of h_{FE_o} and early failure.

The h_{ie} Parameter

The normalized h_{ie} are shown in Figure 27. The discussion in paragraph 5.1.1 concerning the h_{ie} Parameter applies to the general similarities between Figures 25 and 27.

There appeared to be no annealing of h_{ie} during periods of no irradiation. This was in contrast to the 75°C specimens.

5.3 TYPE S2N1486 TRANSISTOR

Ten specimens were irradiated in a controlled temperature chamber adjusted to 30 ± 2°C. However, gamma heating during the latter part of the test caused the temperature to rise above the design limits. Figure 11 shows the temperature trace for these specimens. Note that the rise in temperature occurred well after failure of all the specimens.

5.3.1 The h_{FE} Parameter

Figure 28 shows the normalized h_{FE} data for these specimens. The significant contribution of gamma rays to the degradiation of h_{FE} is again evidenced by the slope discontinuity of the median at the point of shield removal.

The failure pattern for the group is shown in Figure 29. These transistors showed a comparatively low radiation tolerance. All failed before 6×10^{10} n/cm^2 had been accumulated. Initial values of h_{FE} and order of failure were:

h_{FE_o}	Order of Failure
32.32	9
32.88	3
33.84	4
35.00	10
35.18	8
37.44	7
39.60	5
39.97	2
42.09	1
44.38	6

These data show a slight correlation between high values of h_{FE_o} and early failure.

5.3.2 The h_{ie} Parameter

The normalized h_{ie} data for these specimens are shown in Figure 30. The general similarities between Figures 28 and 30 may be explained by the remarks of paragraph 5.1.1 concerning the h_{ie} Parameter.

5.4 TYPE S2N2412 TRANSISTOR

Twenty specimens manufactured by Texas Instruments were irradiated in a controlled temperature chamber adjusted to 30 ± 2°C. During the latter part of the test the temperature rose above the designed limits because of gamma heating. Figure 12 shows the temperature trace for these specimens.

5.4.1 The h_{FE} Parameter

The normalized h_{FE} data for the specimens are shown in Figure 31.

A significant contribution by the gamma component of the irradiation to the degradation of h_{FE} is evidenced by the slope discontinuity in the median at the point of shield removal.

The failure (50% degradation of h_{FE}) pattern for the group is shown in Figure 32. Initial values of h_{FE} and order of failure were:

h_{FE_o}	Order of Failure
52.22	19
54.87	20
56.04	6
61.29	4
64.48	17
69.92	10
70.69	12
74.43	3
74.56	7
74.97	16

h_{FE_o}	Order of Failure (Continued)
74.97	13
79.14	9
80.42	2
80.94	14
85.77	8
85.80	18
87.65	1
97.13	15
99.02	5
112.30	11

These data show no correlation between h_{FE_o} and order of failure.

5.4.2 The h_{ie} Parameter

Figure 33 shows the normalized h_{ie} data for the group. The remarks made in paragraph 5.1.1 concerning the h_{ie} Parameter are applicable to the general similarities between Figures 31 and 33.

5.5 TYPE 2N2498 FIELD EFFECT TRANSISTOR

Twenty-nine specimens manufactured by Texas Instruments were irradiated in a controlled temperature chamber adjusted to hold the temperature at 30 ± 2°C. However, during the latter part of the test, gamma heating caused the temperature to rise above the designed limits. The temperature data for the specimens are shown in Figure 12.

The wide variations in radiation exposure among the specimens necessitated some

compromises in the analyses of the data obtained. The methods used in data analysis and presentation are explained in Section 4.0.

5.5.1 The I_{DSS} Parameter

The I_{DSS} data obtained are shown in Figure 34. This parameter remained essentially constant up to an exposure of 10^{13} n/cm^2, but after this point I_{DSS} declined steadily and reached essentially zero at 1.7×10^{15} n/cm^2. The post-test readings (66 hours later) showed no annealing.

5.5.2 The V_P Parameter

Figure 35 presents the V_P data for these specimens. V_P showed a slight decline before the LiH shield was removed. After removal of the shield V_P slowly increased to about its original value at 2×10^{13} n/cm^2 then began to decrease. After the 15 hour shutdown period irradiation was continued at a reactor power of 3 megawatts. During this period V_P increased, rapidly at first, then more slowly. However, measurements taken immediately after reactor shutdown showed a mean V_P value of about 1 volt. This would indicate that the increase in V_P was a radiation rate effect probably due to leakage within the specimen. The post-test measurements (66 hours later) showed a slight annealing of the V_P parameter. Also, a slight annealing was noted during the 15 hour shutdown period.

V_P data for one unusual specimen are shown in Figure 36.

5.5.3 Transconductance Parameters

Two transconductance measurements were made:

(a) g_{m_o} was measured at $V_{GS} = 0$, $V_{DS} \cong 15V$, and $I_D = I_{DSS}$ ($V_{gs} \cong 50$ mV), and

(b) g_{m_1} at $I_D = 350\mu A$, $V_{DS} \cong 15$ VDC.

The g_{m_o} Parameter

Figure 37 portrays the g_{m_o} data. A small discontinuity in the slope of the mean was noted at the point of shield removal indicating that the gamma component of the irradiation contributed to the degradation of g_{m_o}. A steady decrease in g_{m_o} began at about 4×10^{13} n/cm^2 and continued until g_{m_o} reached almost zero at 1.7×10^{15} n/cm^2. The post-test measurements (66 hours later) showed no annealing of this parameter.

Failure points for the specimens were determined assuming failure occurred when g_{m_o} was 50% of its pre-test value. The resulting failure pattern is shown in Figure 38.

Initial values of g_{m_o} and order of failure were:

g_{m_o} (μ mhos)	Order of Failure
1857	24
1999	8
2002	16
2016	18
2086	29
2142	2
2187	25
2230	6
2249	1
2274	11
2279	10

g_{m_o} (μmhos)	Order of Failure
	(Continued)
2286	19
2296	20
2319	7
2328	4
2339	14
2341	5
2402	21
2443	9
2456	23
2521	13
2572	17
2644	12
2649	28
2678	22
2695	26
2721	15
2802	27
2976	3

These data show no correlation between initial values of g_{m_o} and order of failure.

The g_{m_1} Parameter

The g_{m_1} data are shown in Figure 39. The general behavior of this parameter was more constant during irradiation than g_{m_o}, probably because of the constant I_D. Note that g_{m_1} falls off only slightly up to the point where I_D falls above the degradated I_{DSS}. No useable data were obtained beyond 5×10^{14} n/cm^2 as I_D could not be maintained at 350μA for all specimens beyond this point.

TABLE 1 TEST SPECIMENS AND TEST CONDITIONS

Board Number	Description	Number	Test Conditions	Parameter	Remarks
1	Transistor, 2N708 NPN, Si, Fairchild	20	V_{CE} = 1V, I_C = 10mA	h_{FE}	75°C
			V_{CE} = 1V, I_C = 10mA I_B = 10μA at 1kc	h_{ie}	
2	Transistor, 2N708 NPN, Si, Fairchild	20	V_{CE} = 1V, I_C = 10mA	h_{FE}	30°C
			V_{CE} = 1V, I_C = 10mA I_B = 10μA at 1kc	h_{ie}	
3	Transistor, 2N918 NPN, Si, Fairchild	20	V_{CE} = 1V, I_C = 10mA	h_{FE}	75°C
			V_{CE} = 1V, I_C = 10mA I_B = 10μA at 1kc	h_{ie}	
4	Transistor, 2N918 NPN, Si, Fairchild	20	V_{CE} = 1V, I_C = 10mA	h_{FE}	30°C
			V_{CE} = 1V, I_C = 10mA I_B = 10μA at 1kc	h_{ie}	
5	Transistor, S2N-1486, NPN, Si, Silicon	10	V_{CE} = 4V, I_C = 750mA	h_{FE}	30°C
			V_{CE} = 4V, I_C = 750mA I_B = 15mA at 1kc	h_{ie}	
6	Transistor, S2N-2412, PNP, Si, Texas Instrument	20	V_{CE} = 5V, I_C = 10mA	h_{FE}	30°C
			V_{CE} = 5V, I_C = 10mA I_B = 10μA at 1kc	h_{ie}	
7 & 8	Transistor, 2N-2498, P Channel, Si, Texas Instruments	29	I_D = 350μA	g_{m_1}	30°C
			V_{GS} = 0, $V_{DS} \cong$ 15V $I_D = I_{DSS}(V_{gs} \cong 50mV)$	g_{m_o}	
			$V_{DS} \cong$ 15V, V_{GS} = 0	I_{DSS}	
			I_D = 3.5μA, $V_{DS} \cong$ 15V	V_P	

TABLE 2 MANUFACTURERS' SPECIFICATIONS FOR TEST SPECIMENS

Type	Conditions	Specification
2N708	V_{CE} = 1V, I_C = 10mA, T = 25°C	h_{FE} = 30 min., pulsed
2N918	V_{CE} = 3V, I_C = 30mA, T = 25°C	h_{FE} = 20 min.
S2N1486	V_{CE} = 4V, I_C = 750mA, T = 25°C	h_{FE} = 35 to 100
S2N2412	V_{CE} = 0.5V, I_C = 10mA, T = 25°C	h_{FE} = 55
2N2498	I_D = 2.0mA	h_o = 1500 μmhos min.

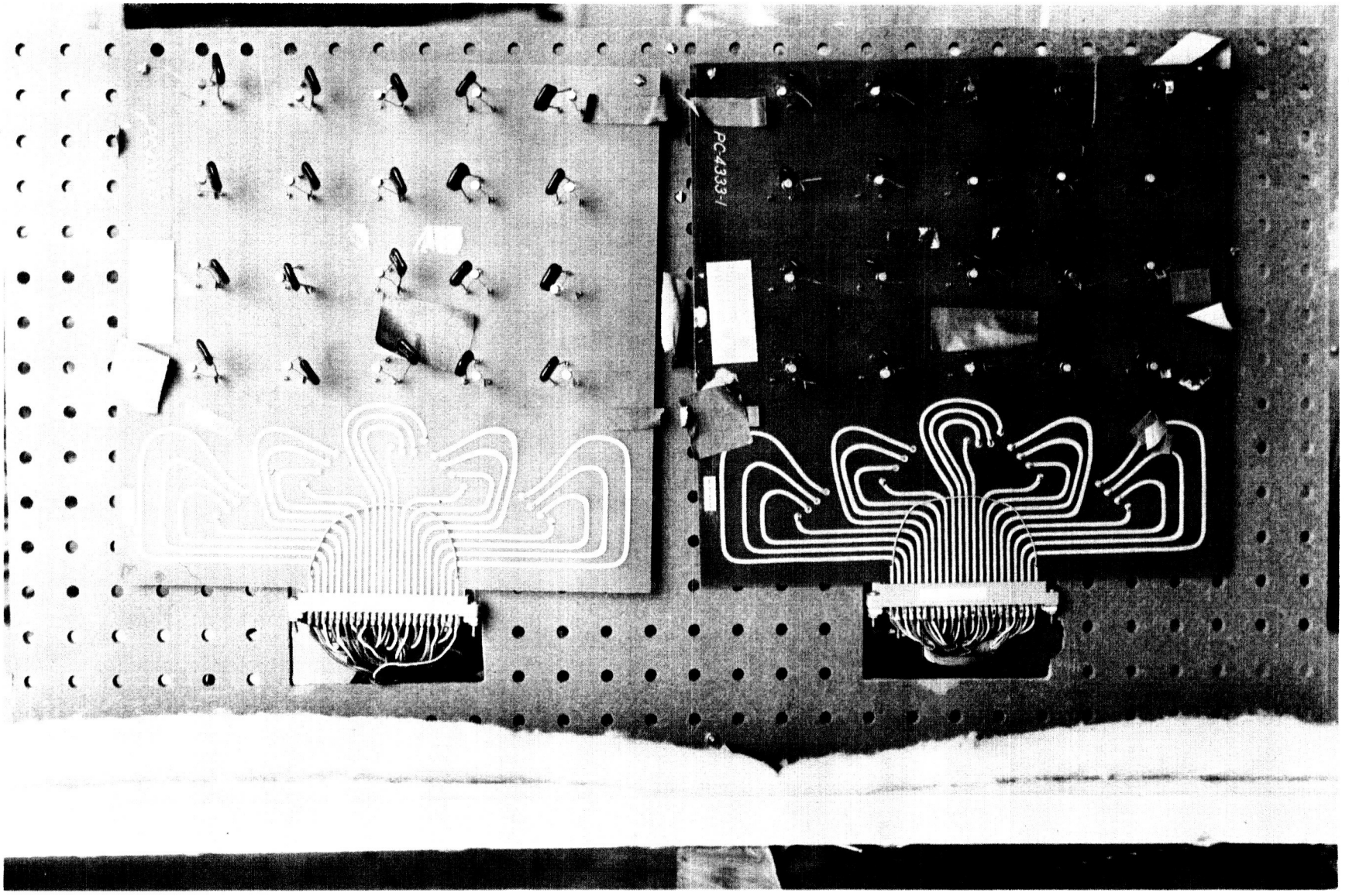

FIGURE 1 SPECIMEN BOARDS 1 AND 3 AS SEEN FROM REACTOR

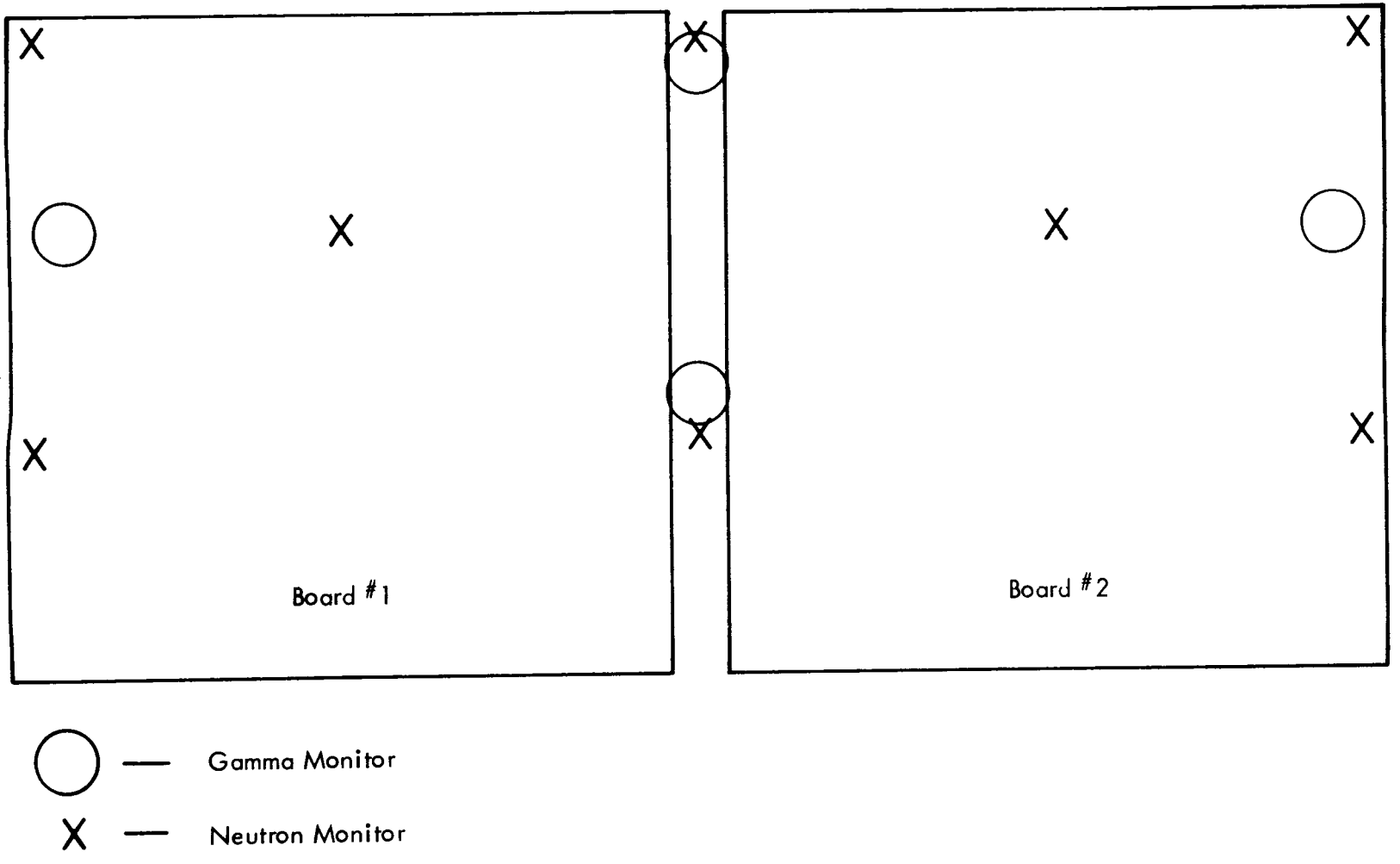

FIGURE 2 DIAGRAM OF SPECIMEN BOARDS 1 AND 3 AS SEEN FROM REACTOR

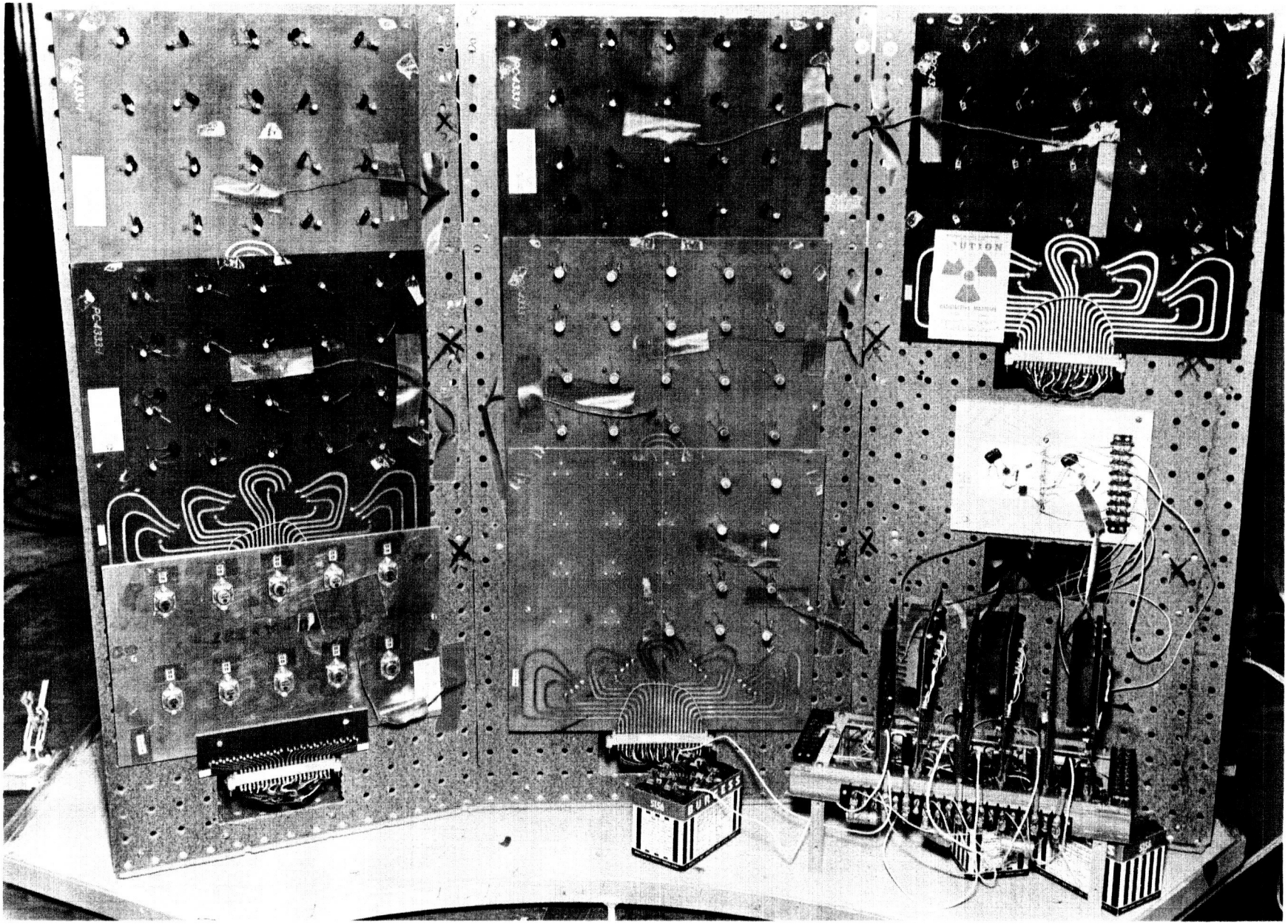

FIGURE 3 TEST PANEL AS SEEN FROM REACTOR

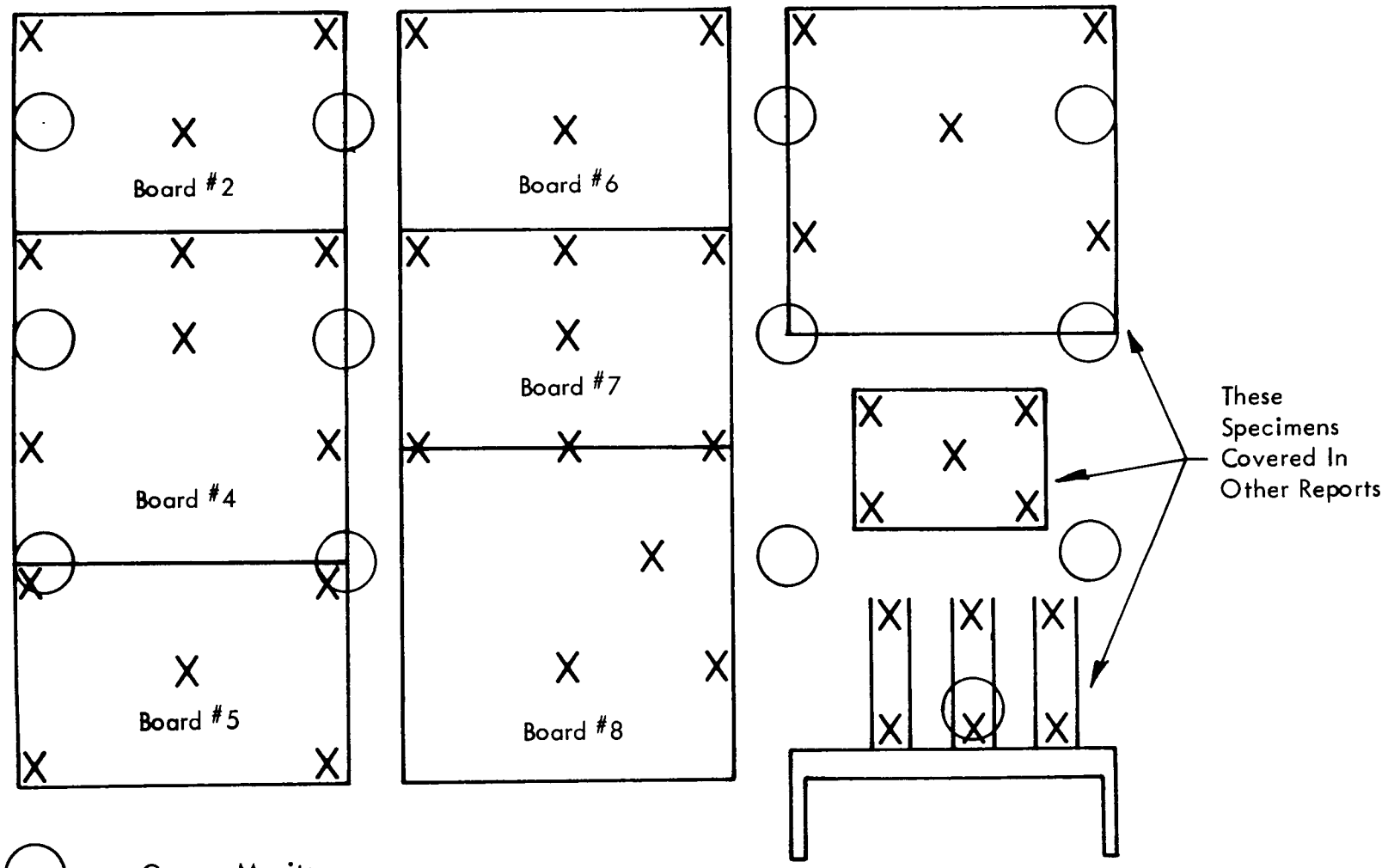

FIGURE 4 DIAGRAM OF TEST PANEL AS SEEN FROM REACTOR

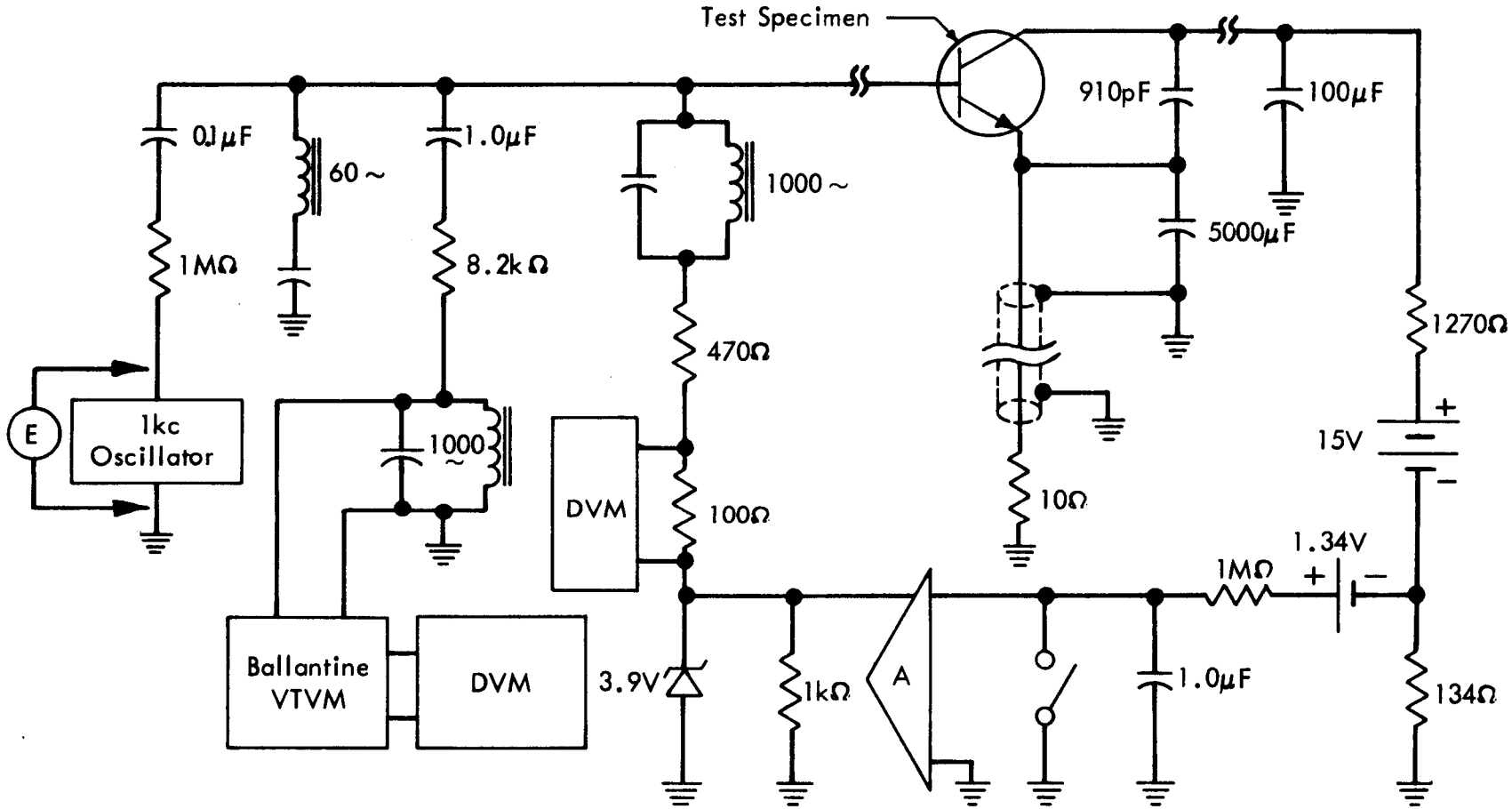

Parameter	I_C	V_{CE}	E
h_{FE}	10mA	1V	0
h_{ie}	10mA	1V	10V

FIGURE 5 2N708 AND 2N918 MEASUREMENT CIRCUIT

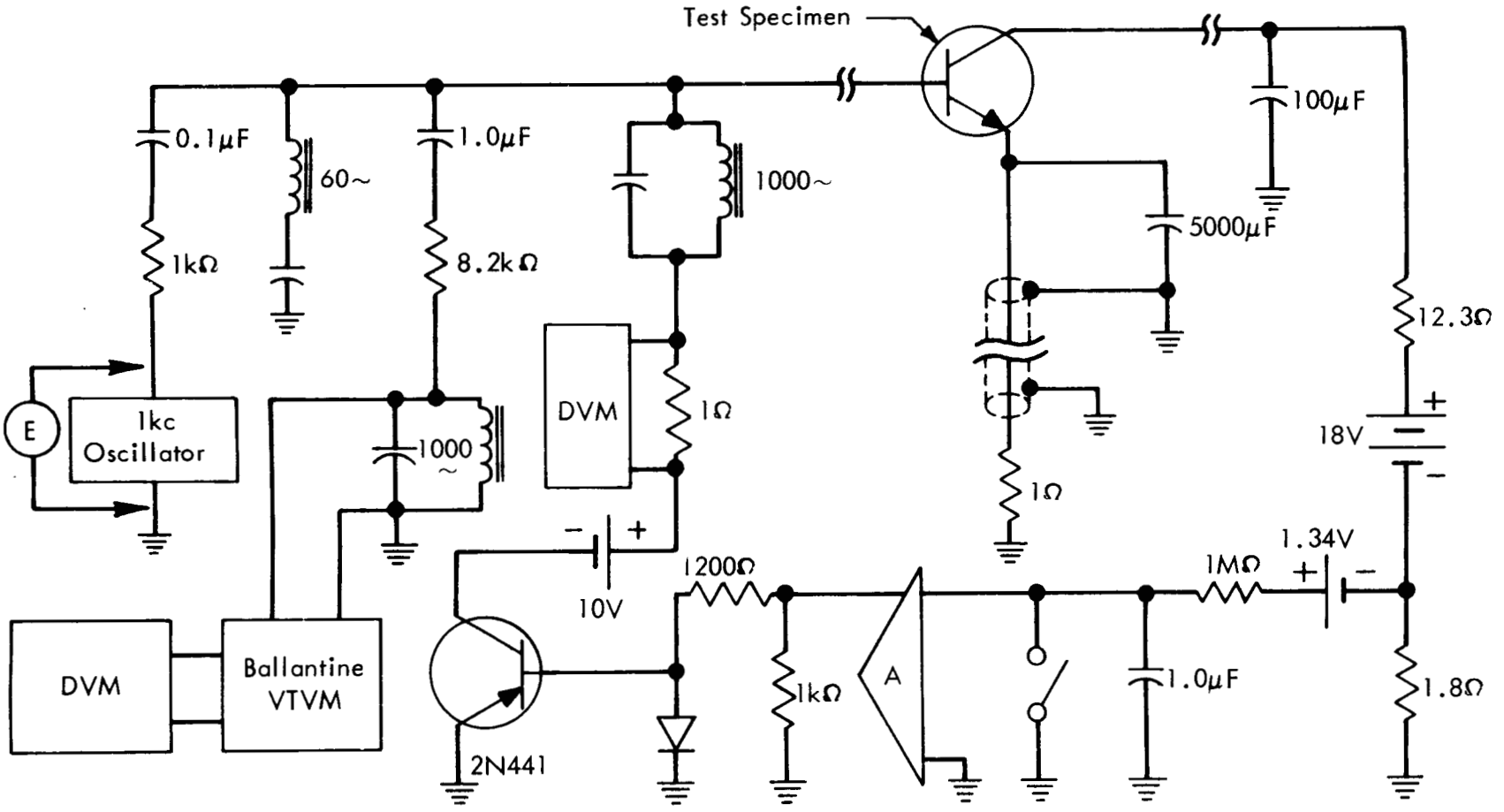

Parameter	I_C	V_{CE}	E
h_{FE}	750mA	4V	0
h_{ie}	750mA	4V	15V

FIGURE 6 S2N1486 MEASUREMENT CIRCUIT

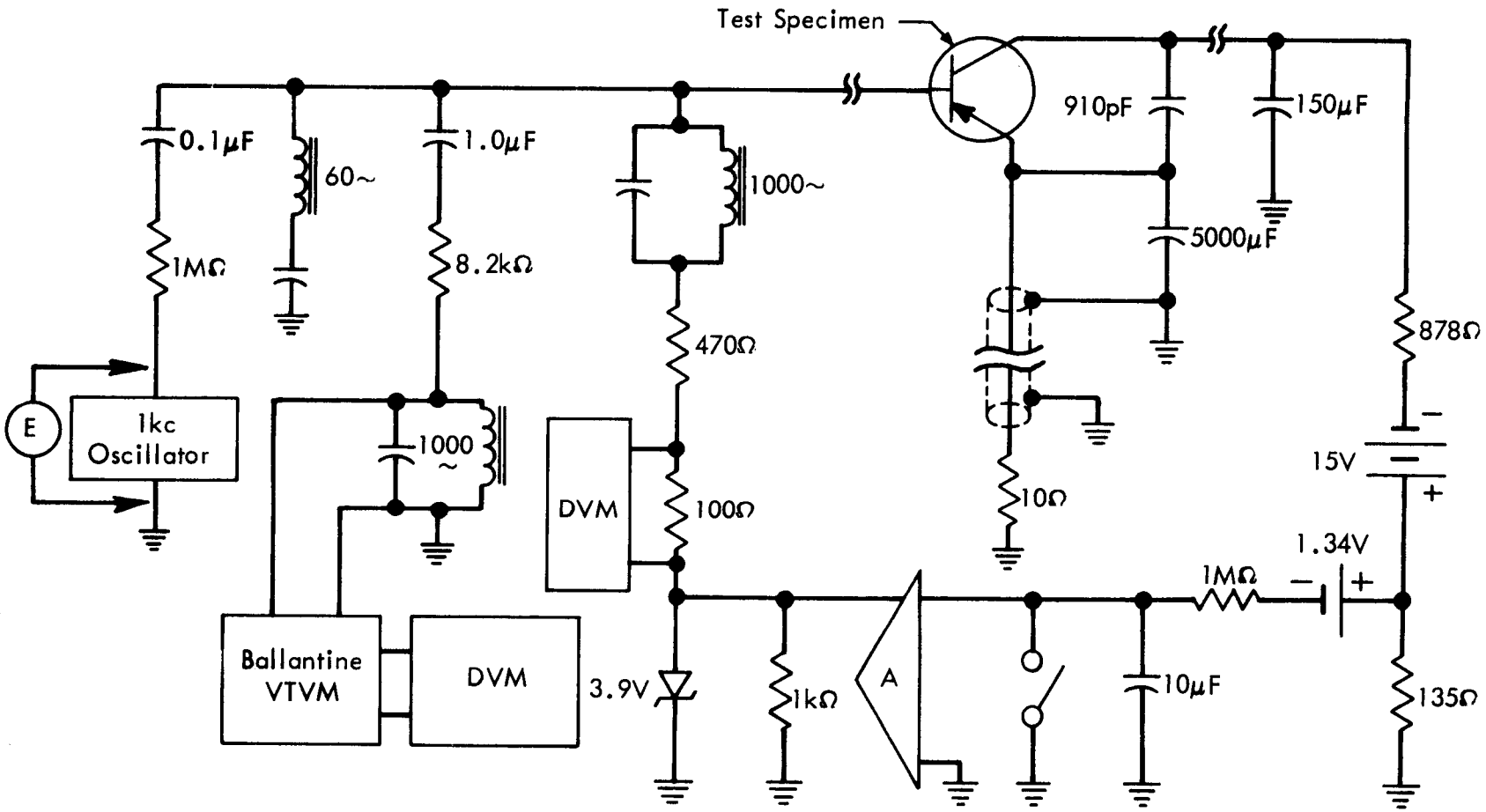

Parameter	I_C	V_{CE}	E
h_{FE}	10mA	5V	0
h_{ie}	10mA	5V	10V

FIGURE 7 S2N2412 (PNP) MEASUREMENT CIRCUIT

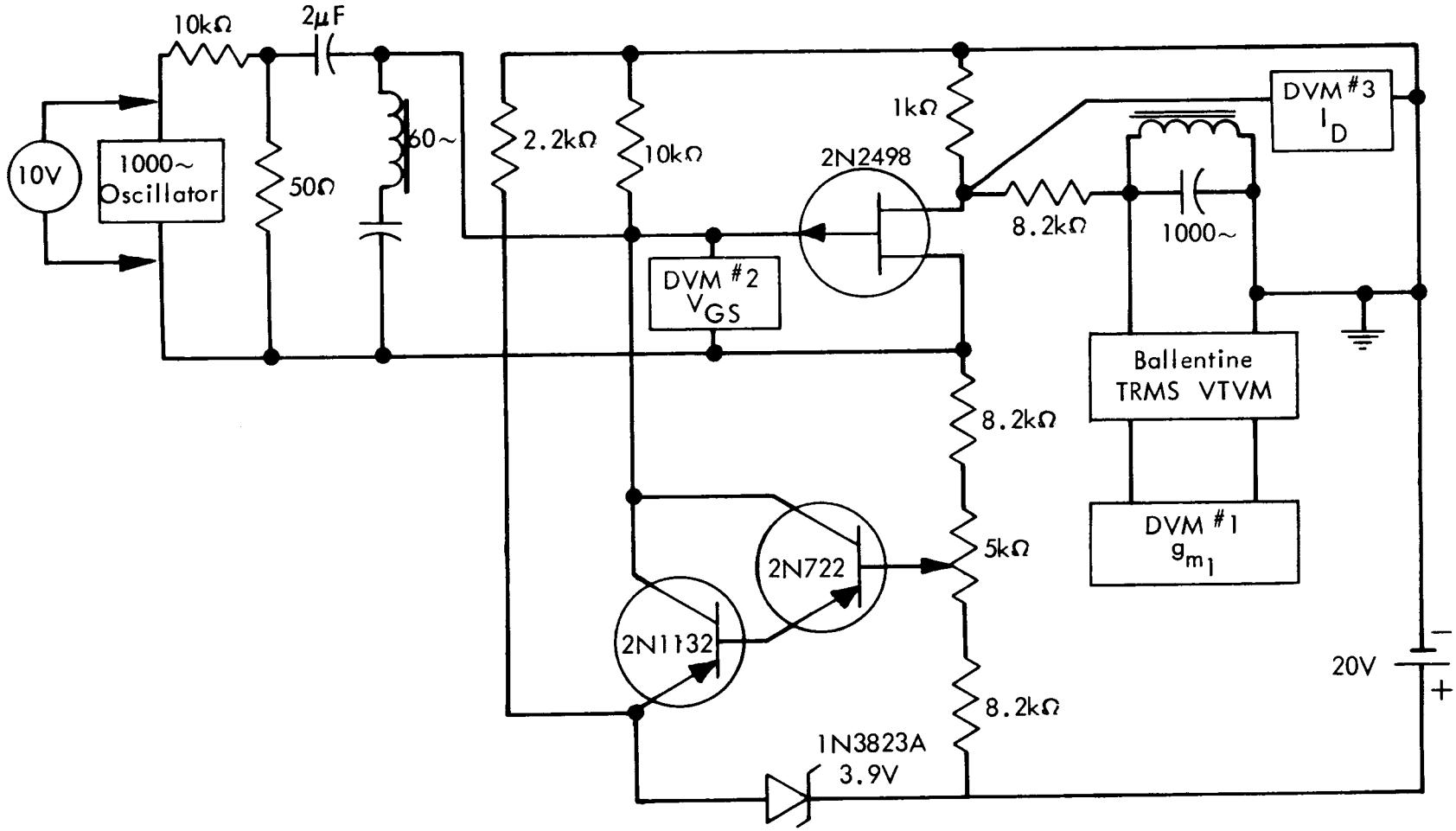

$I_D = 0.1\ I_{DSS}$ ($I_{DSS} = 3.5$mA)

$V_{DS} \cong 15$VDC

FIGURE 8 TRANSCONDUCTANCE MEASUREMENTS FOR FIELD EFFECT TRANSISTORS

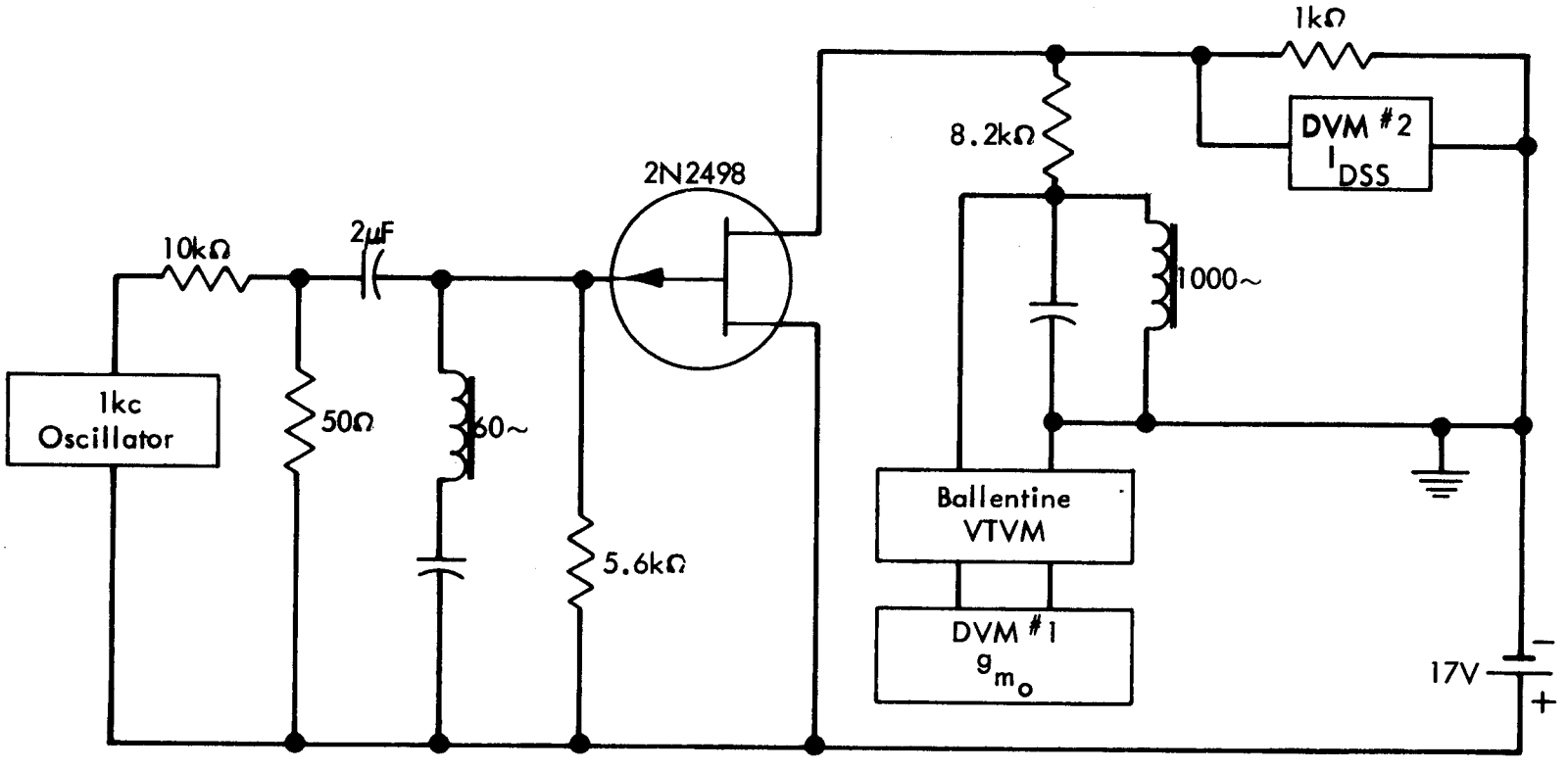

$V_{GS} = 0$

$I_D = I_{DSS}$ ($V_{gs} \cong 50mV$)

$V_{DS} = \cong 15V$

FIGURE 9 TRANSCONDUCTANCE MEASUREMENTS FOR FIELD EFFECT TRANSISTORS

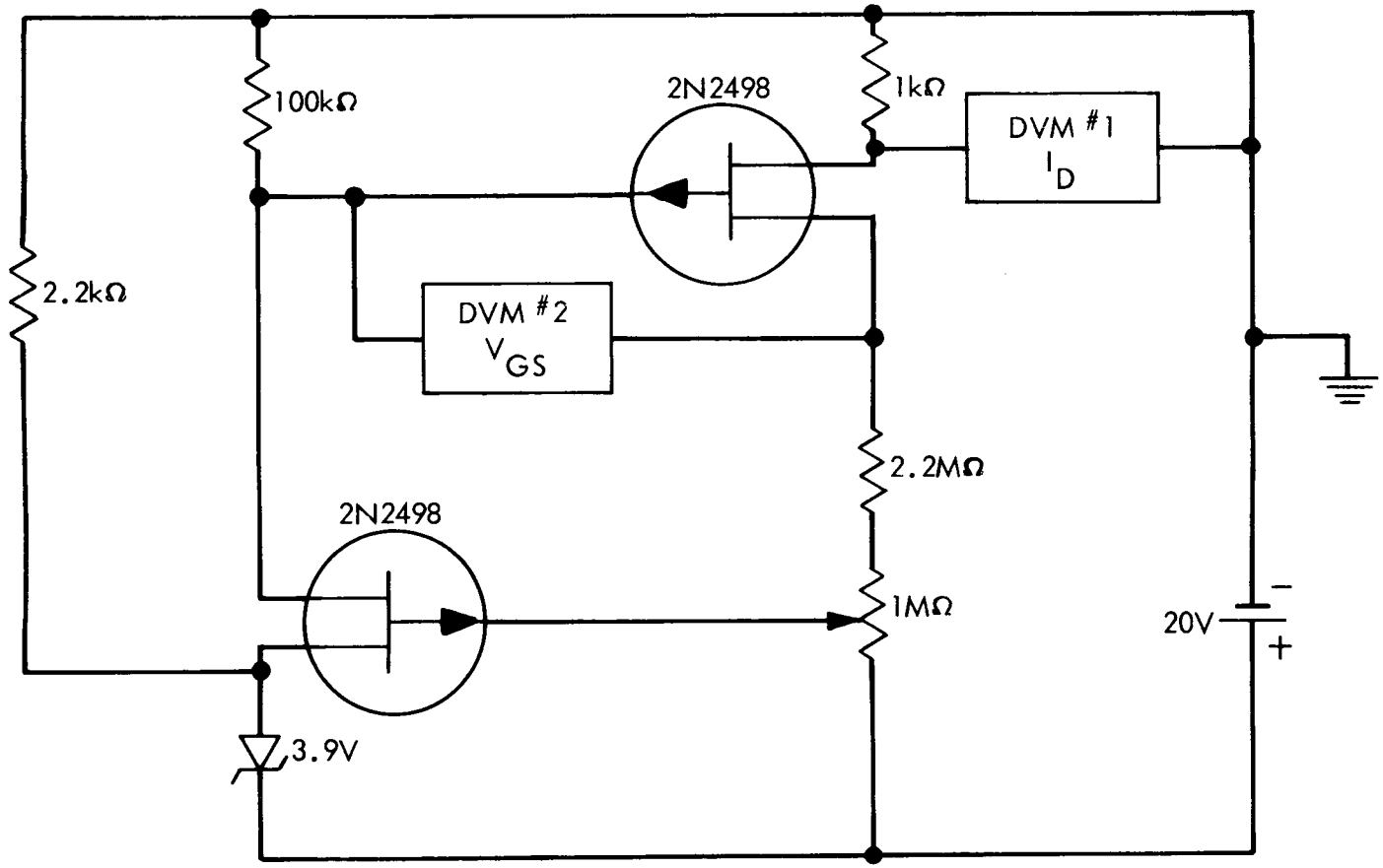

$I_D = .001\ I_{DSS}\ (3.5\mu A)$

$V_{DS} = \cong 15V$

FIGURE 10 PINCH-OFF VOLTAGE MEASUREMENTS FOR FIELD EFFECT TRANSISTORS

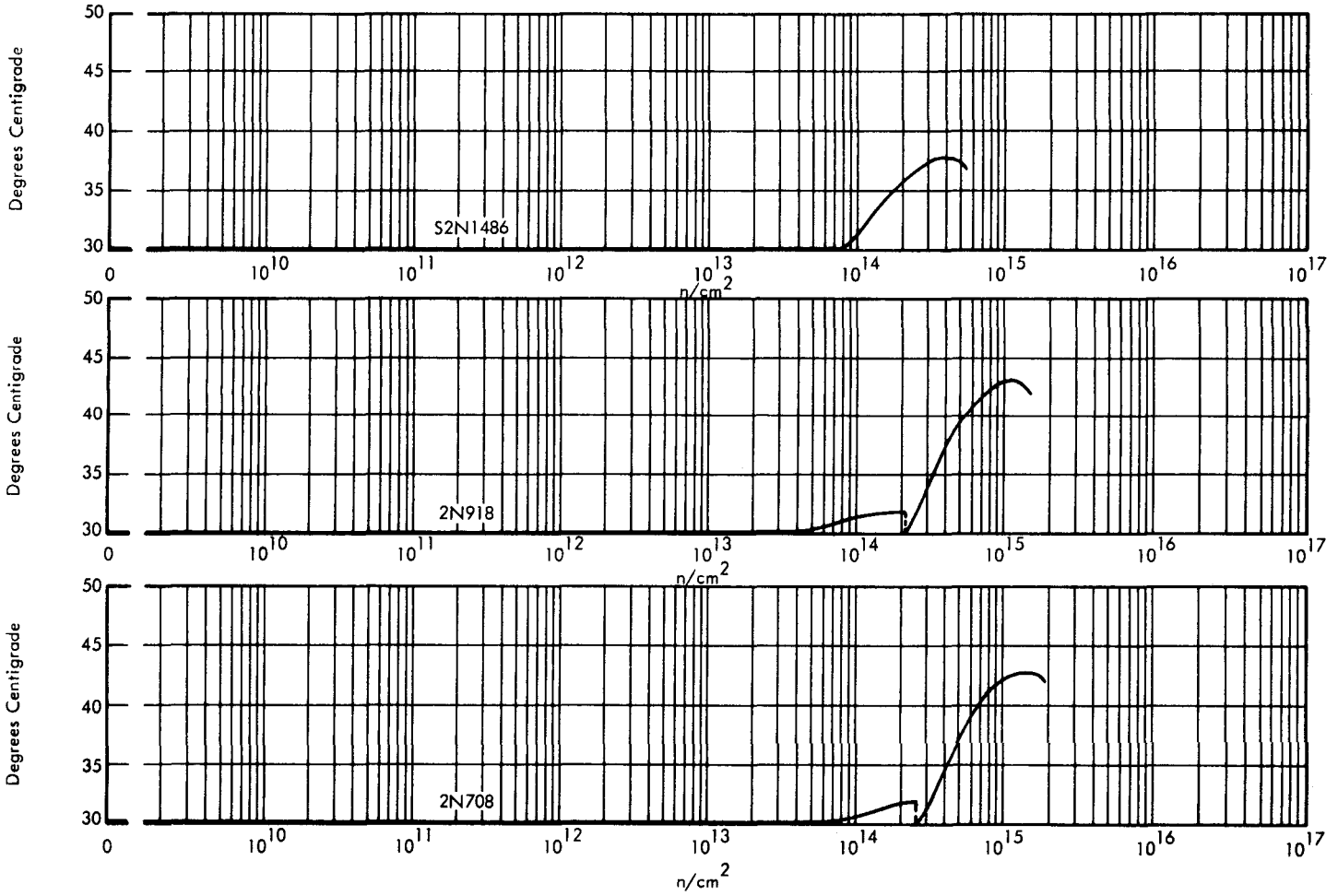

FIGURE 11 TEMPERATURES VERSUS INTEGRATED NEUTRON FLUX

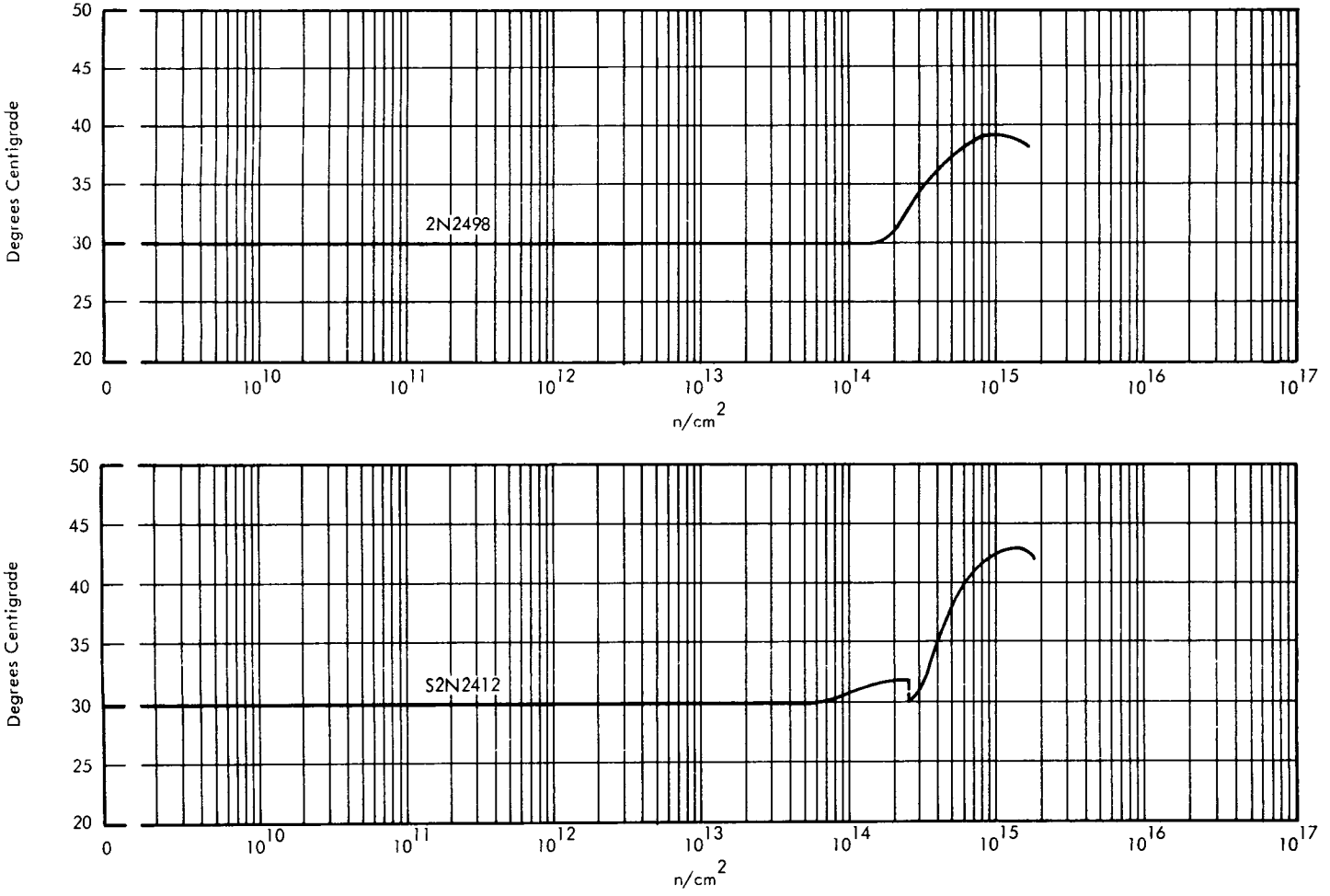

FIGURE 12 TEMPERATURES VERSUS INTEGRATED NEUTRON FLUX

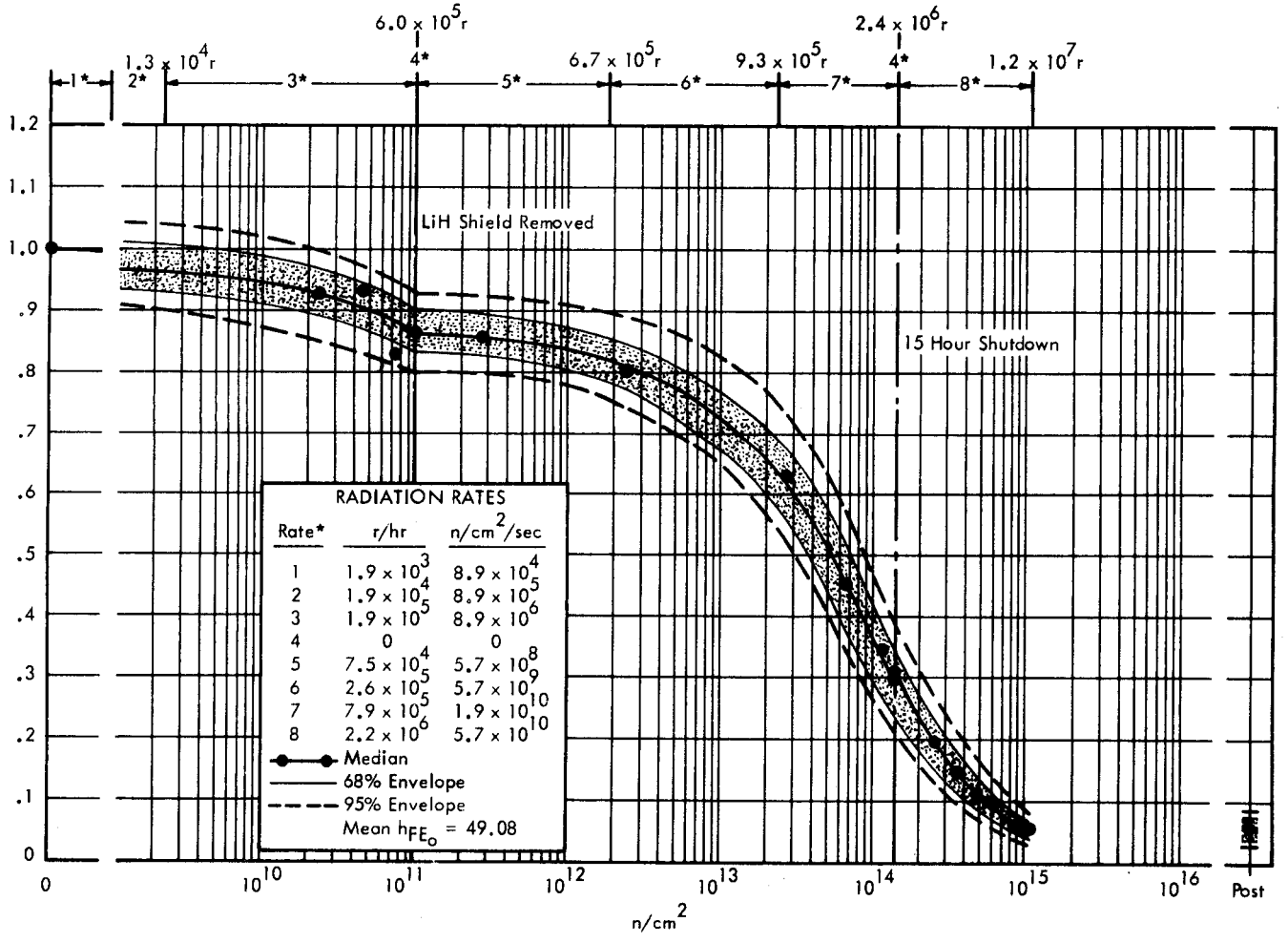

FIGURE 13 2N708 FAIRCHILD, 75°C, NORMALIZED h_{FE} VERSUS INTEGRATED NEUTRON FLUX

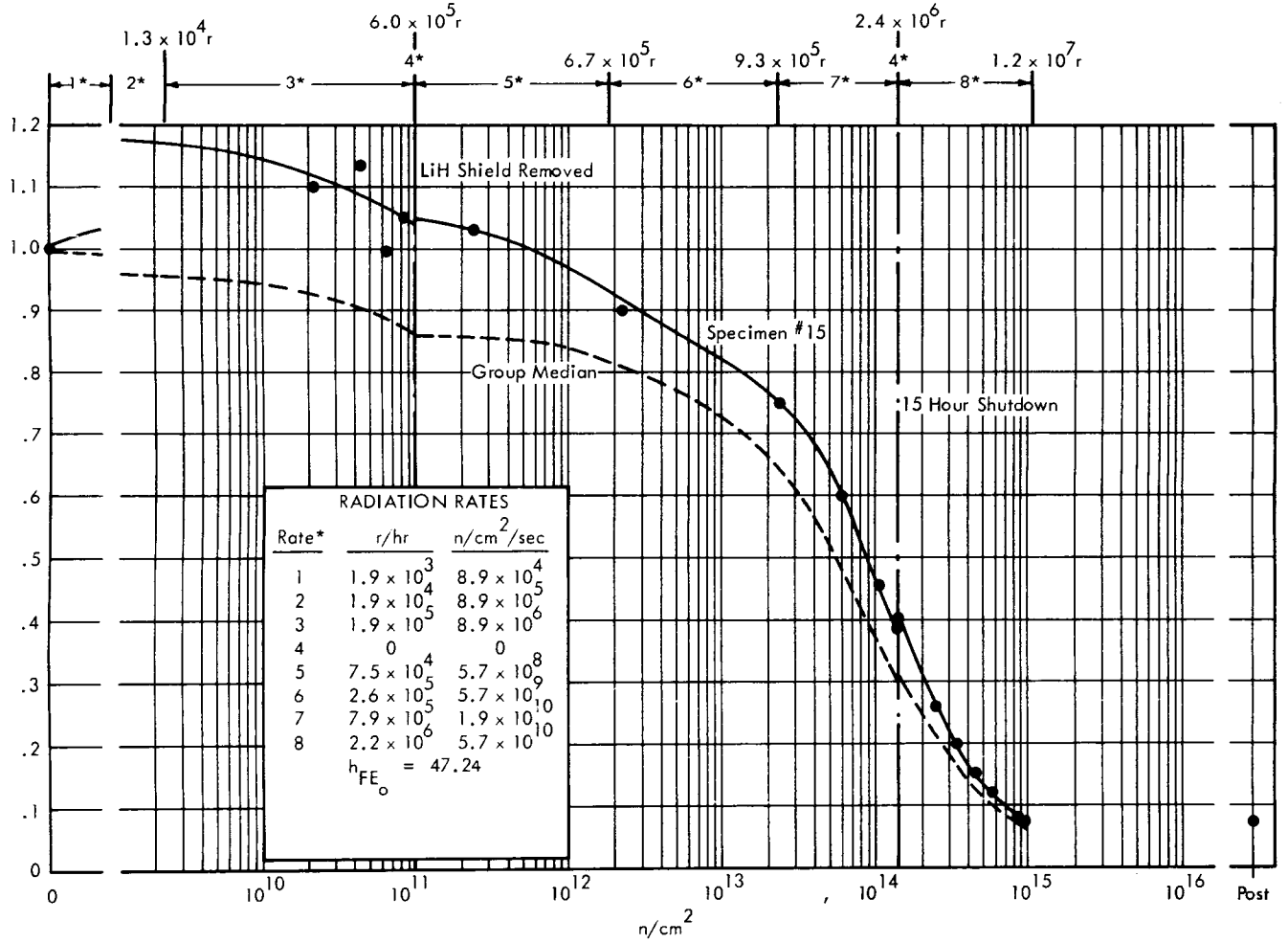

FIGURE 14 2N708 FAIRCHILD, 75°C, ONE UNUSUAL SPECIMEN, NORMALIZED h_{FE} VERSUS INTEGRATED NEUTRON FLUX

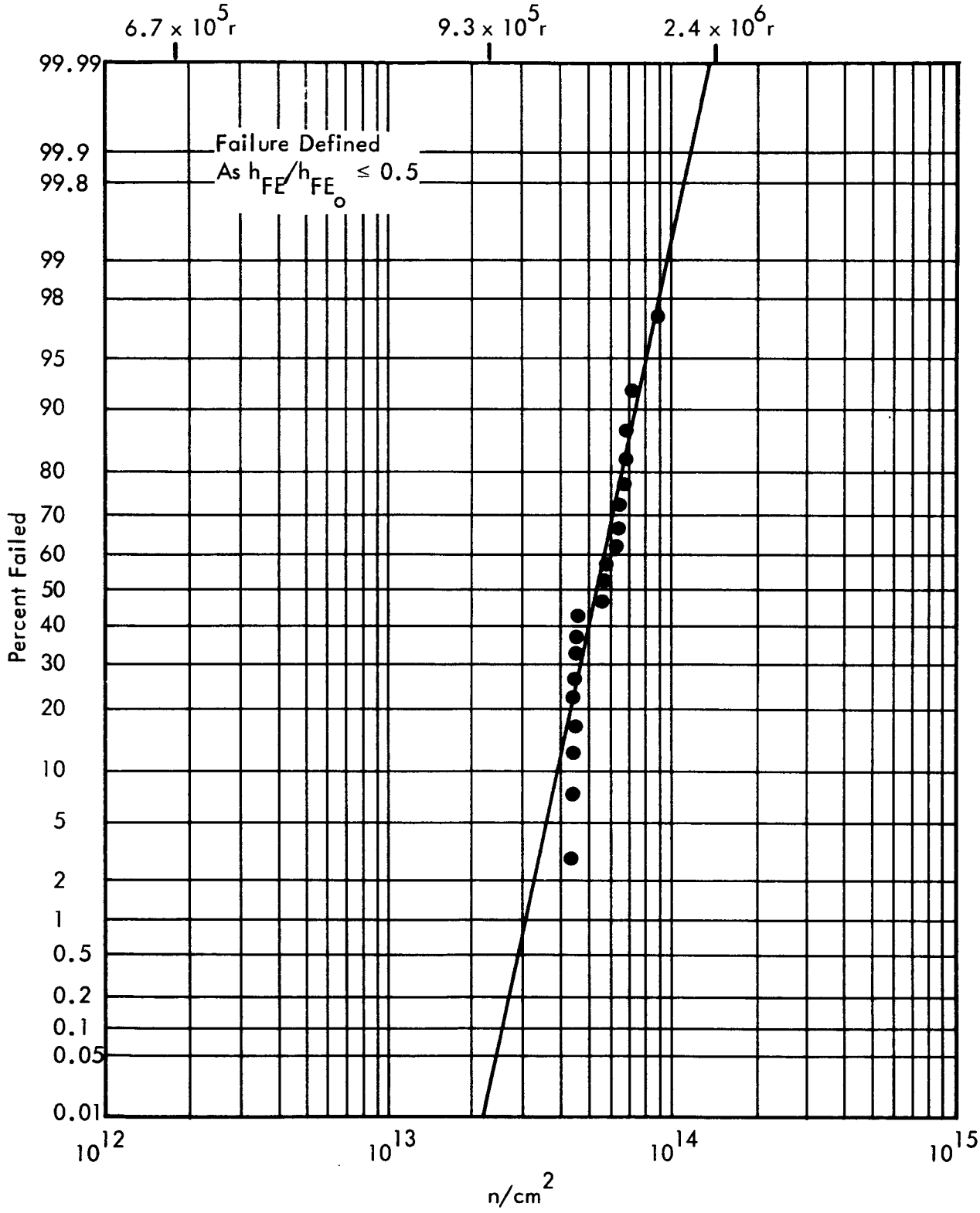

FIGURE 15 2N708 FAIRCHILD, 75°C, PERCENT FAILED VERSUS INTEGRATED NEUTRON FLUX

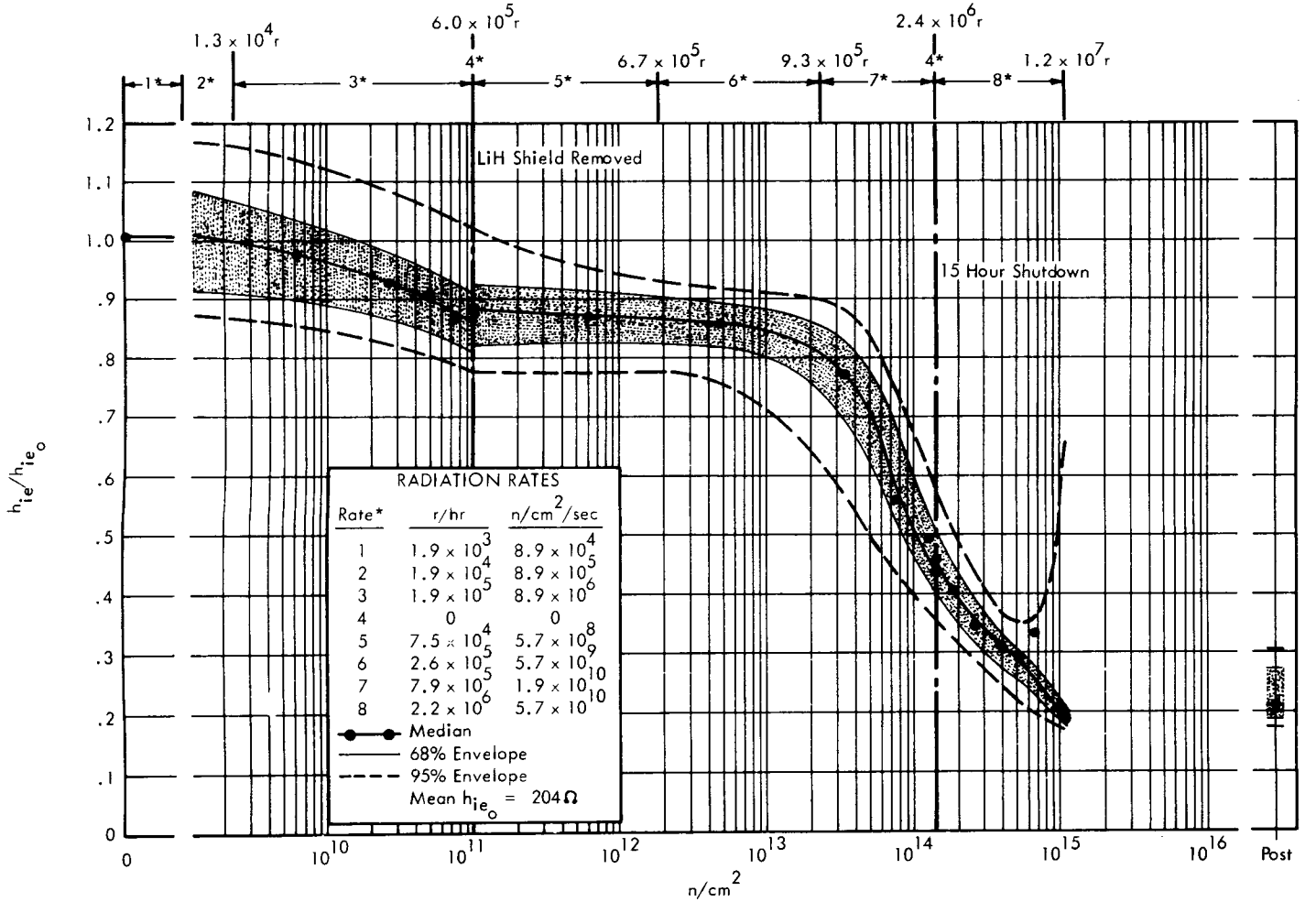

FIGURE 16 2N708 FAIRCHILD, 75°C, NORMALIZED h_{ie} VERSUS INTEGRATED NEUTRON FLUX

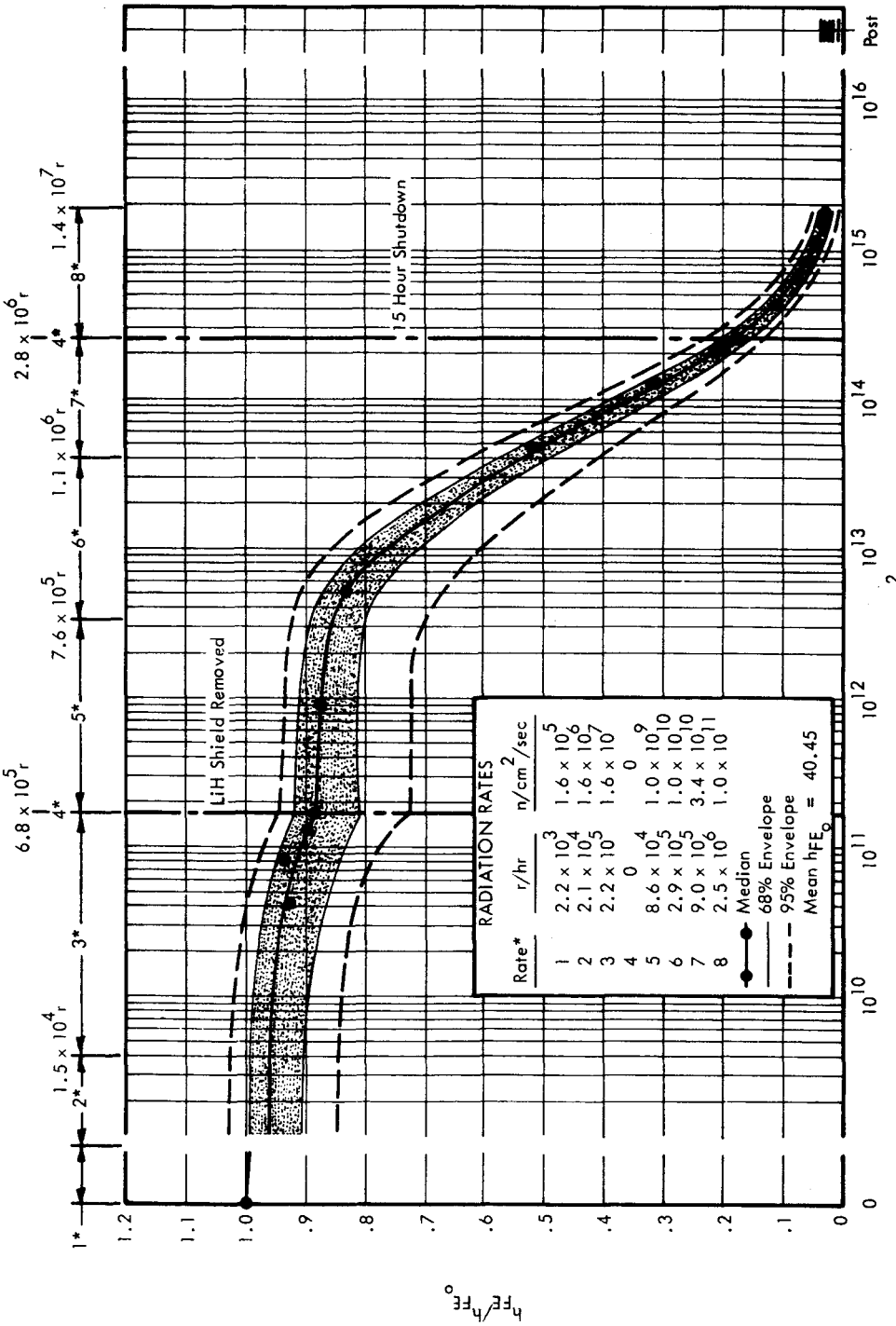

FIGURE 17 2N708 FAIRCHILD, 30°C, NORMALIZED h_{FE} VERSUS INTEGRATED NEUTRON FLUX

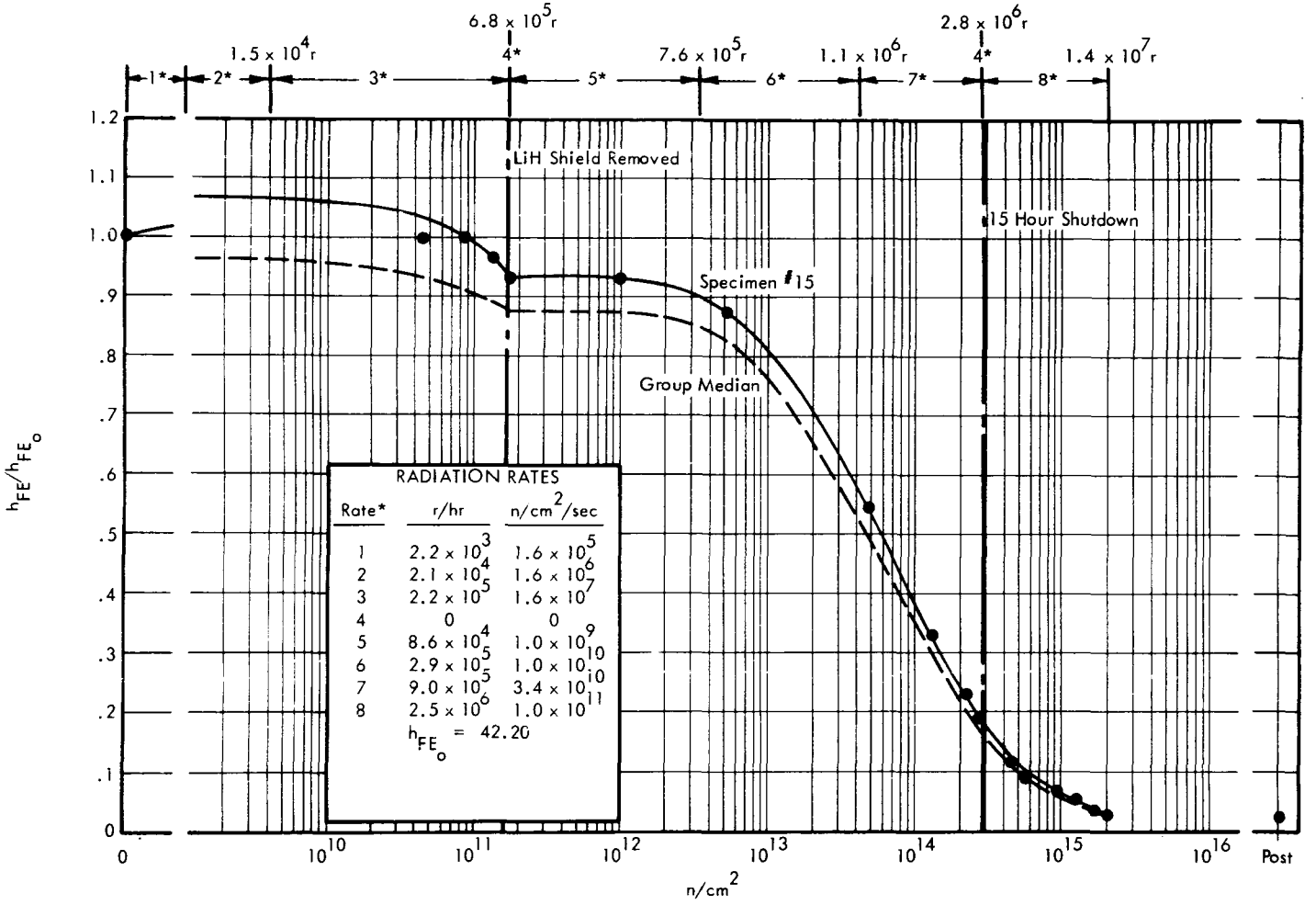

FIGURE 18 2N708 FAIRCHILD, 30°C, ONE UNUSUAL SPECIMEN, NORMALIZED h_{FE} VERSUS INTEGRATED NEUTRON FLUX

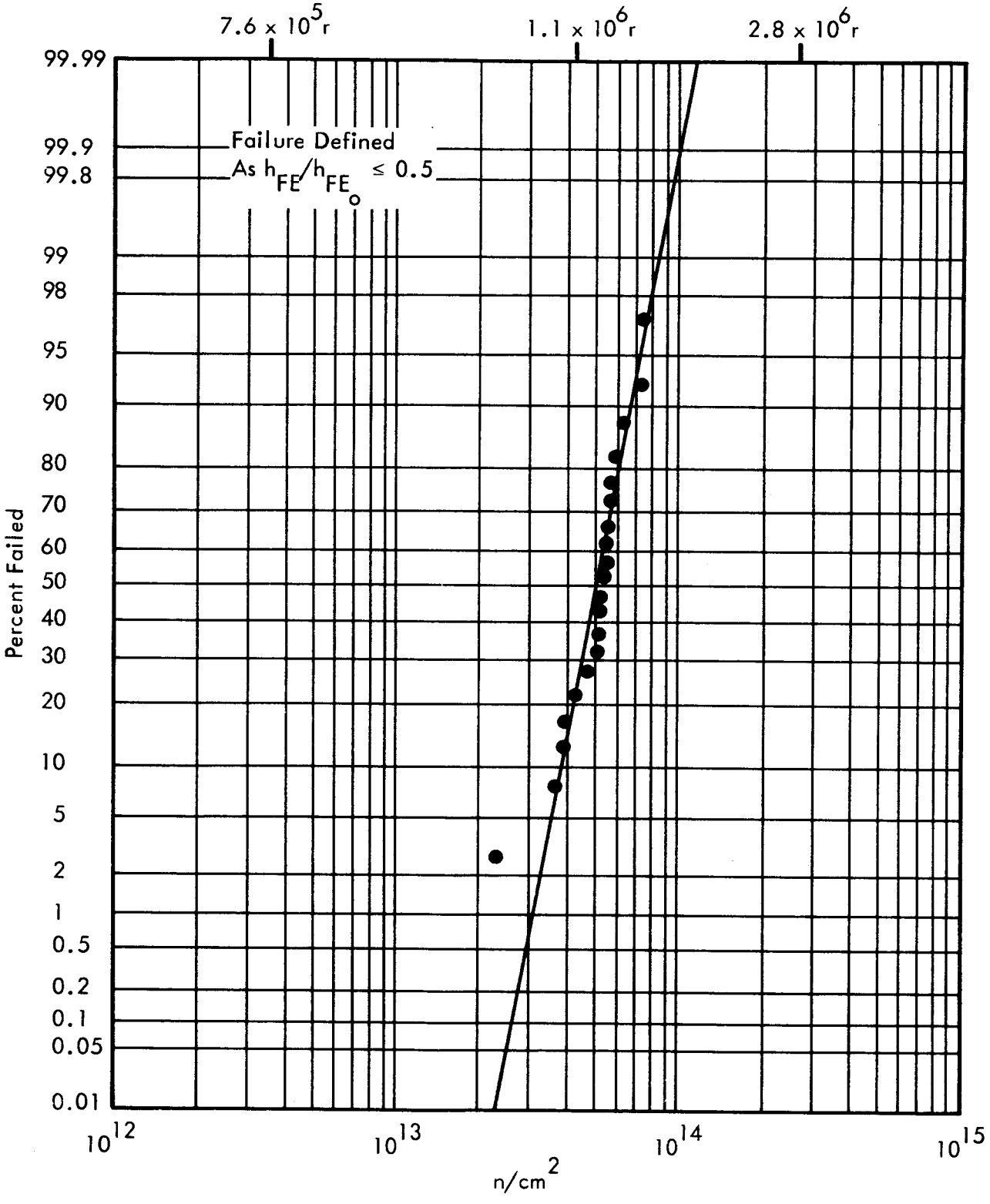

FIGURE 19 2N708 FAIRCHILD, 30°C, PERCENT FAILED VERSUS INTEGRATED NEUTRON FLUX

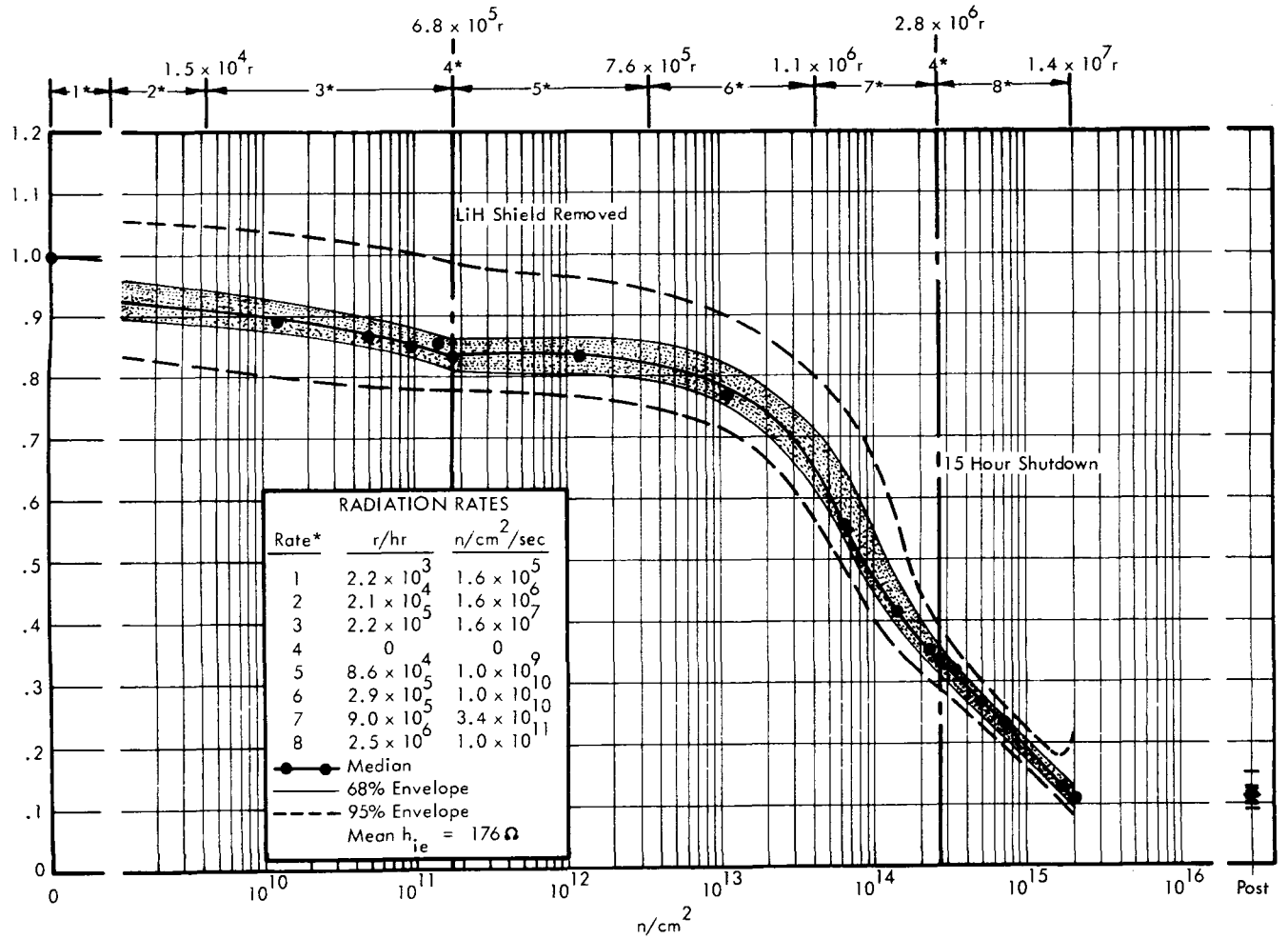

FIGURE 20 2N708 FAIRCHILD, 30°C, NORMALIZED h_{ie} VERSUS INTEGRATED NEUTRON FLUX

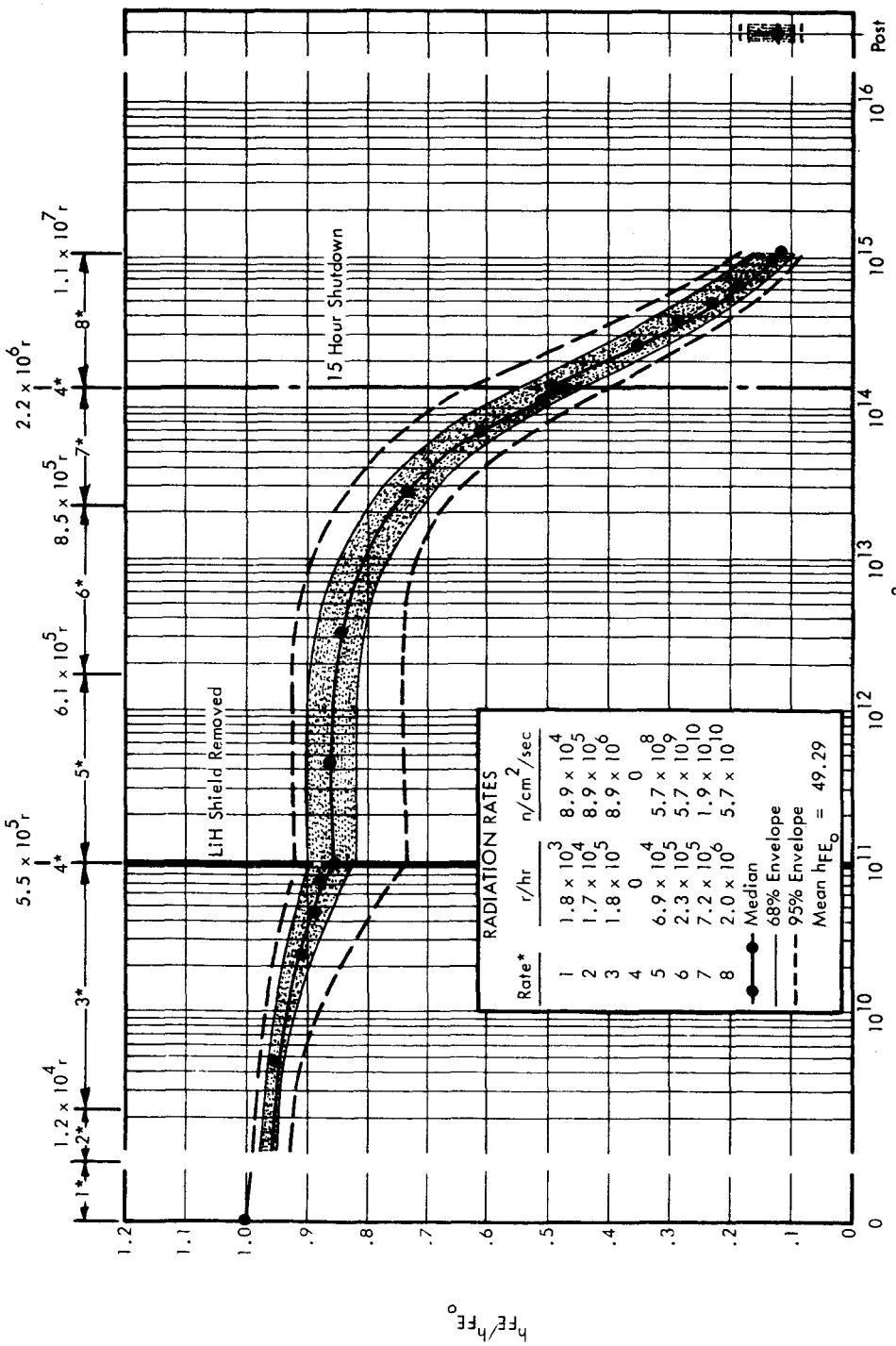

FIGURE 21 2N918 FAIRCHILD, 75°C, NORMALIZED h_{FE} VERSUS INTEGRATED NEUTRON FLUX

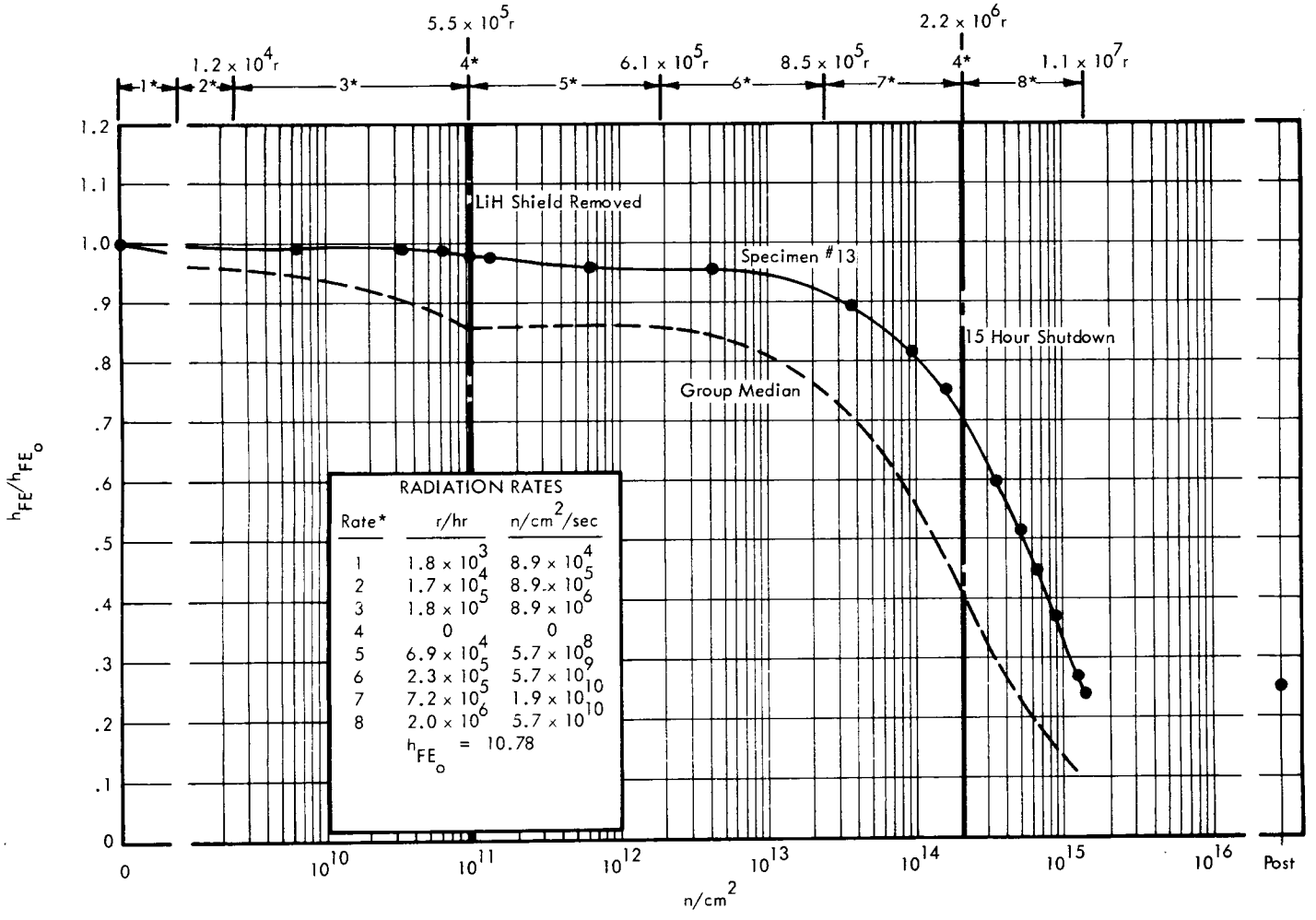

FIGURE 22 2N918 FAIRCHILD, 75°C, ONE UNUSUAL SPECIMEN, NORMALIZED h_{FE} VERSUS INTEGRATED NEUTRON FLUX

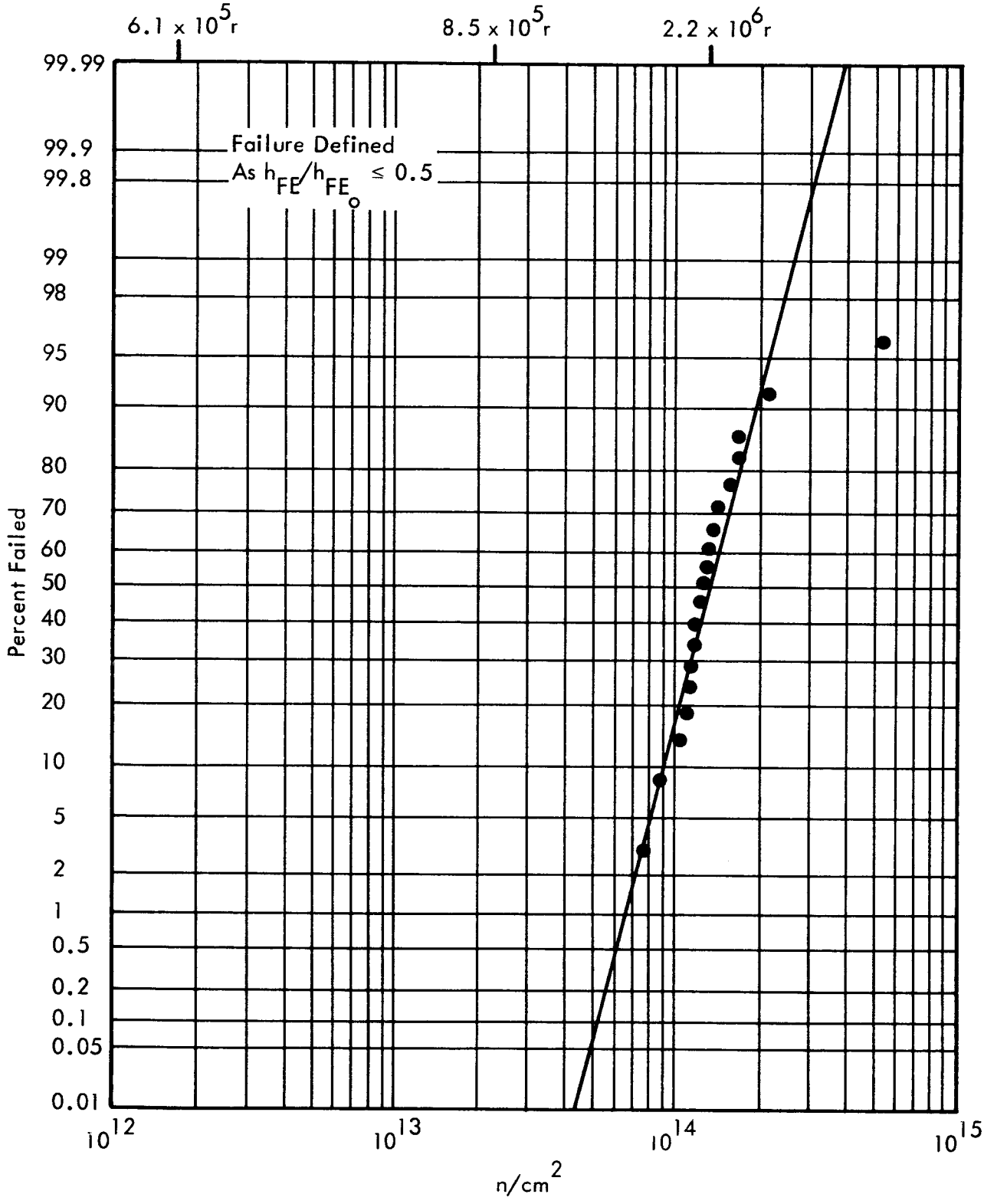

FIGURE 23 2N918 FAIRCHILD, 75°C, PERCENT FAILED VERSUS INTEGRATED NEUTRON FLUX

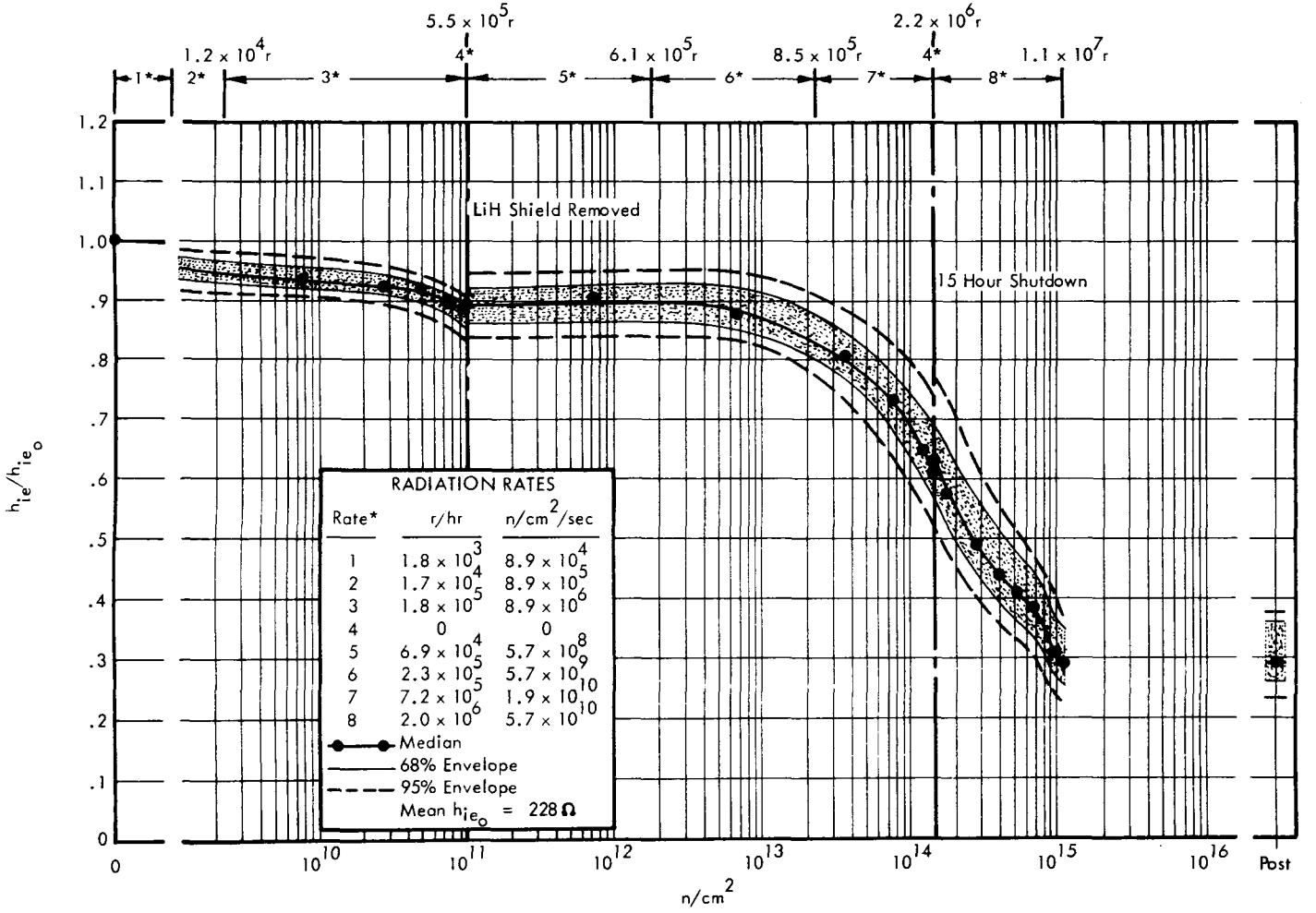

FIGURE 24 2N918 FAIRCHILD, 75°C, NORMALIZED h_{ie} VERSUS INTEGRATED NEUTRON FLUX

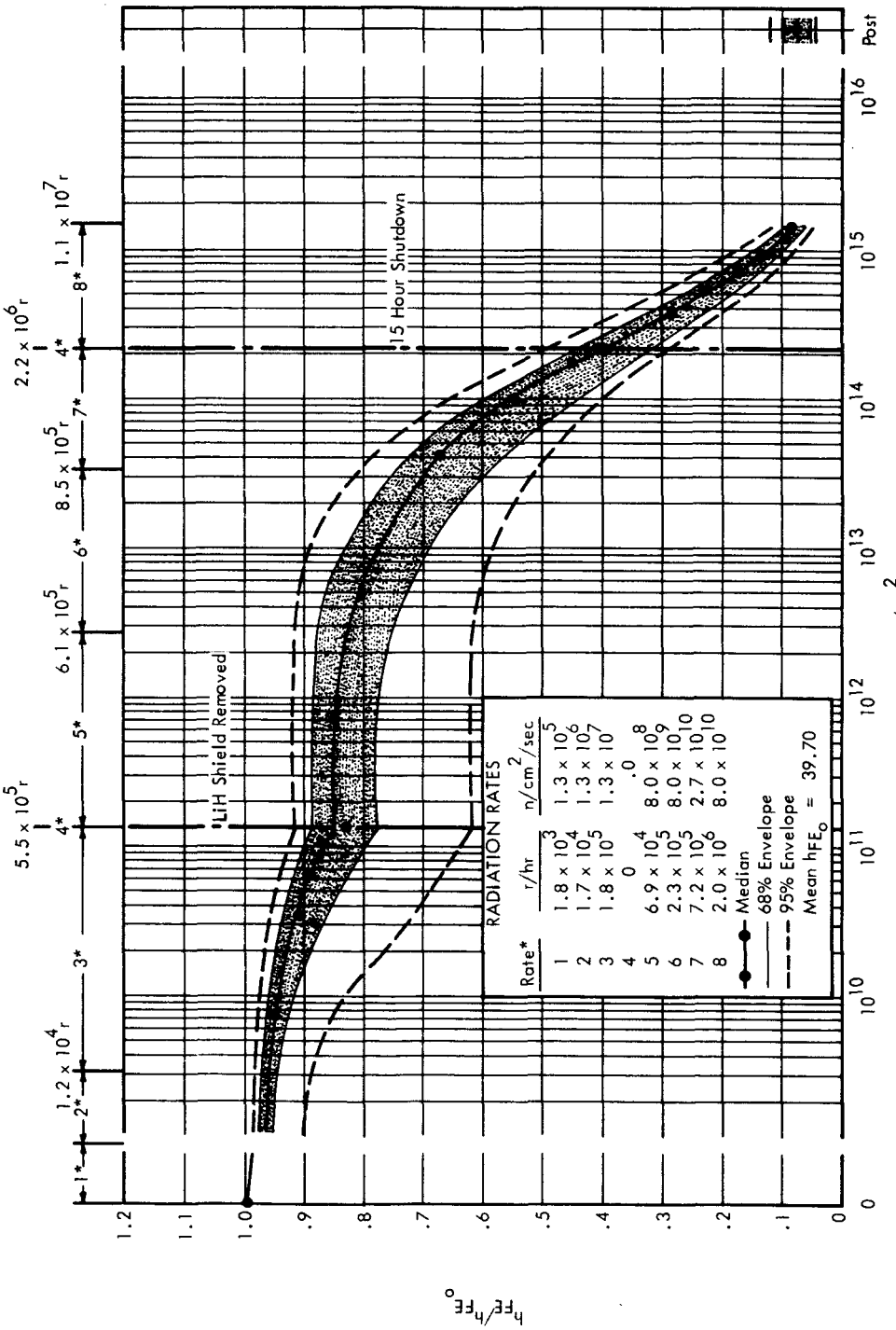

FIGURE 25 2N918 FAIRCHILD, 30°C, NORMALIZED h_{FE} VERSUS INTEGRATED NEUTRON FLUX

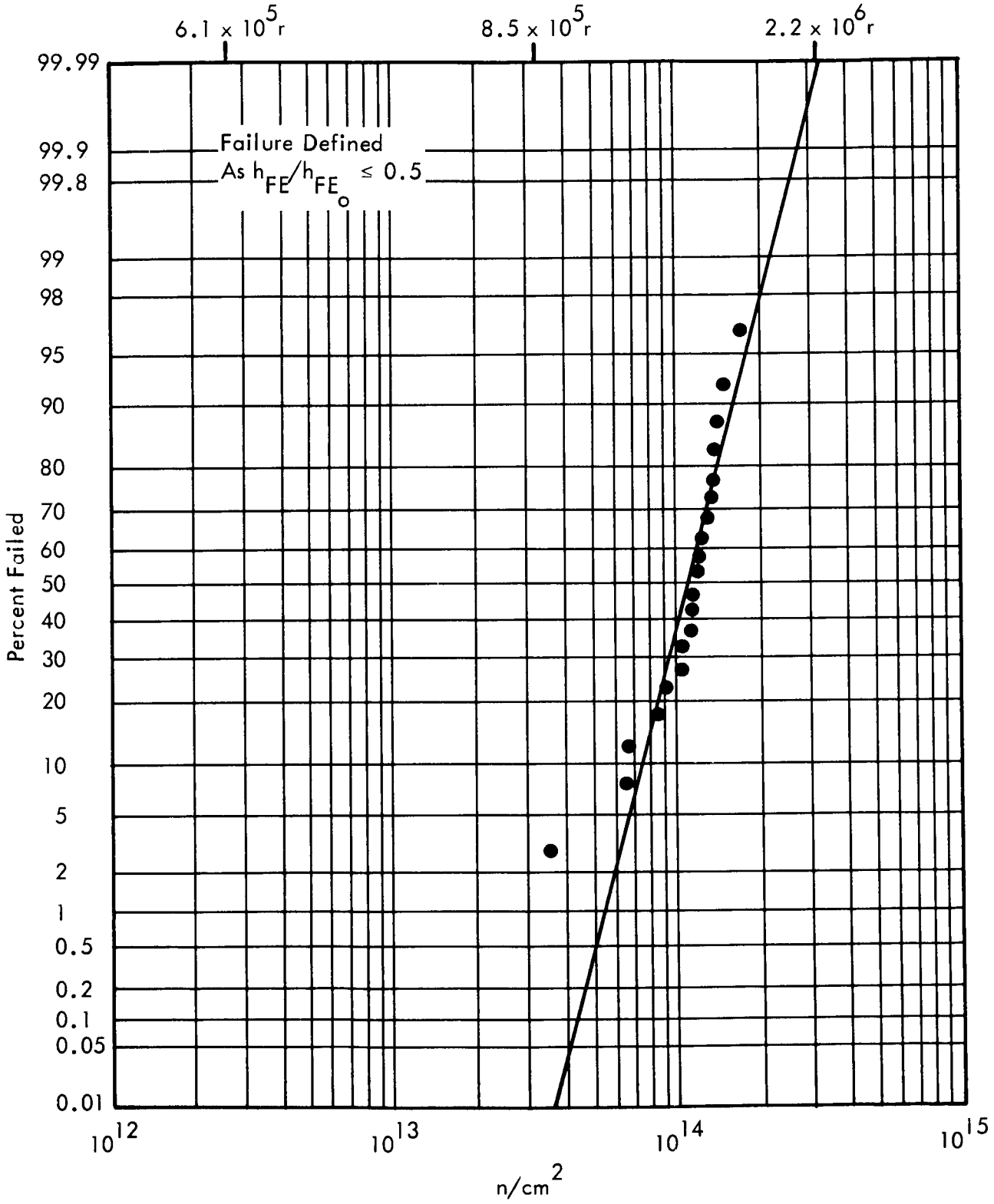

FIGURE 26 2N918 FAIRCHILD, 30°C, PERCENT FAILED VERSUS INTEGRATED NEUTRON FLUX

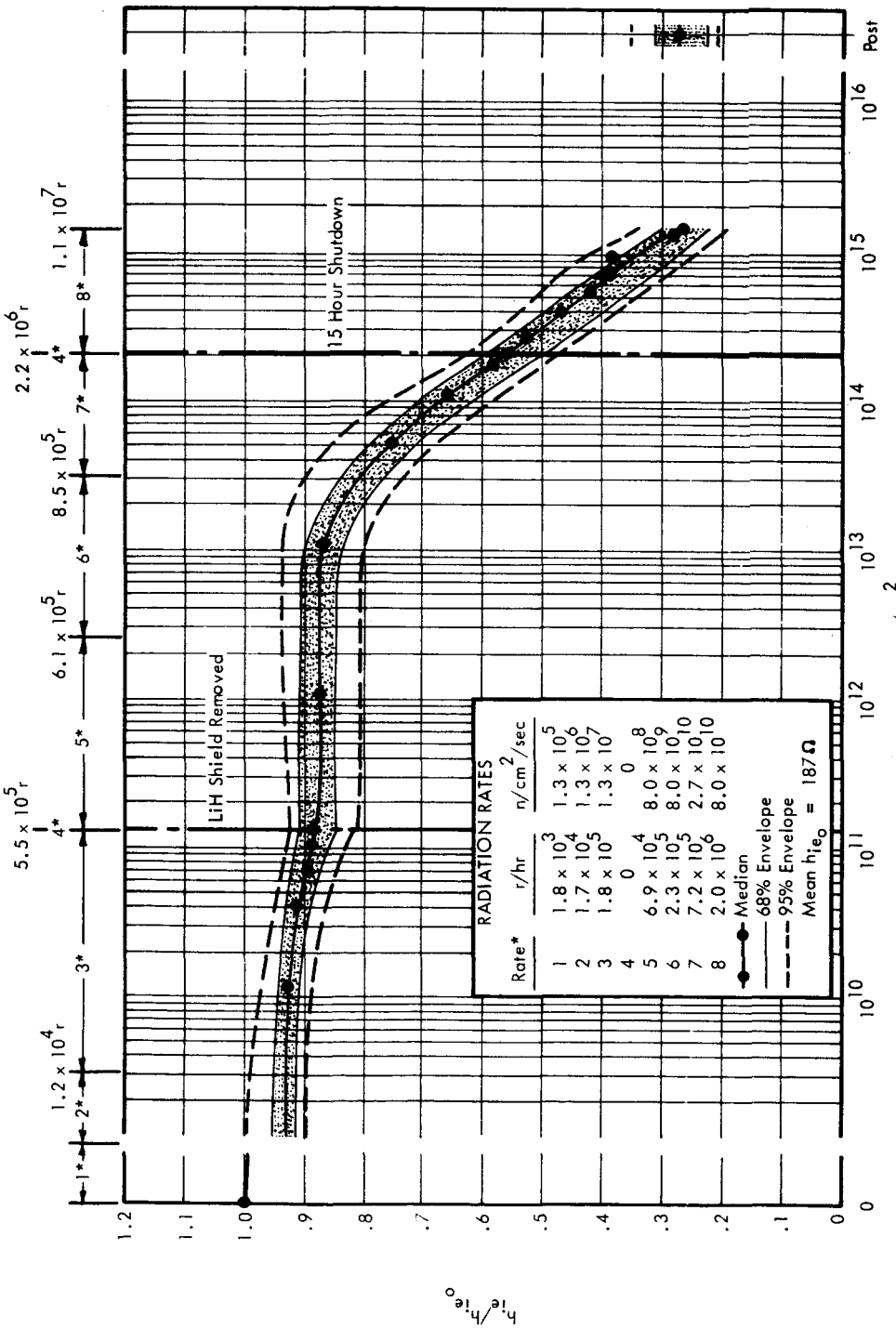

FIGURE 27 2N918 FAIRCHILD, 30°C, NORMALIZED h_{ie} VERSUS INTEGRATED NEUTRON FLUX

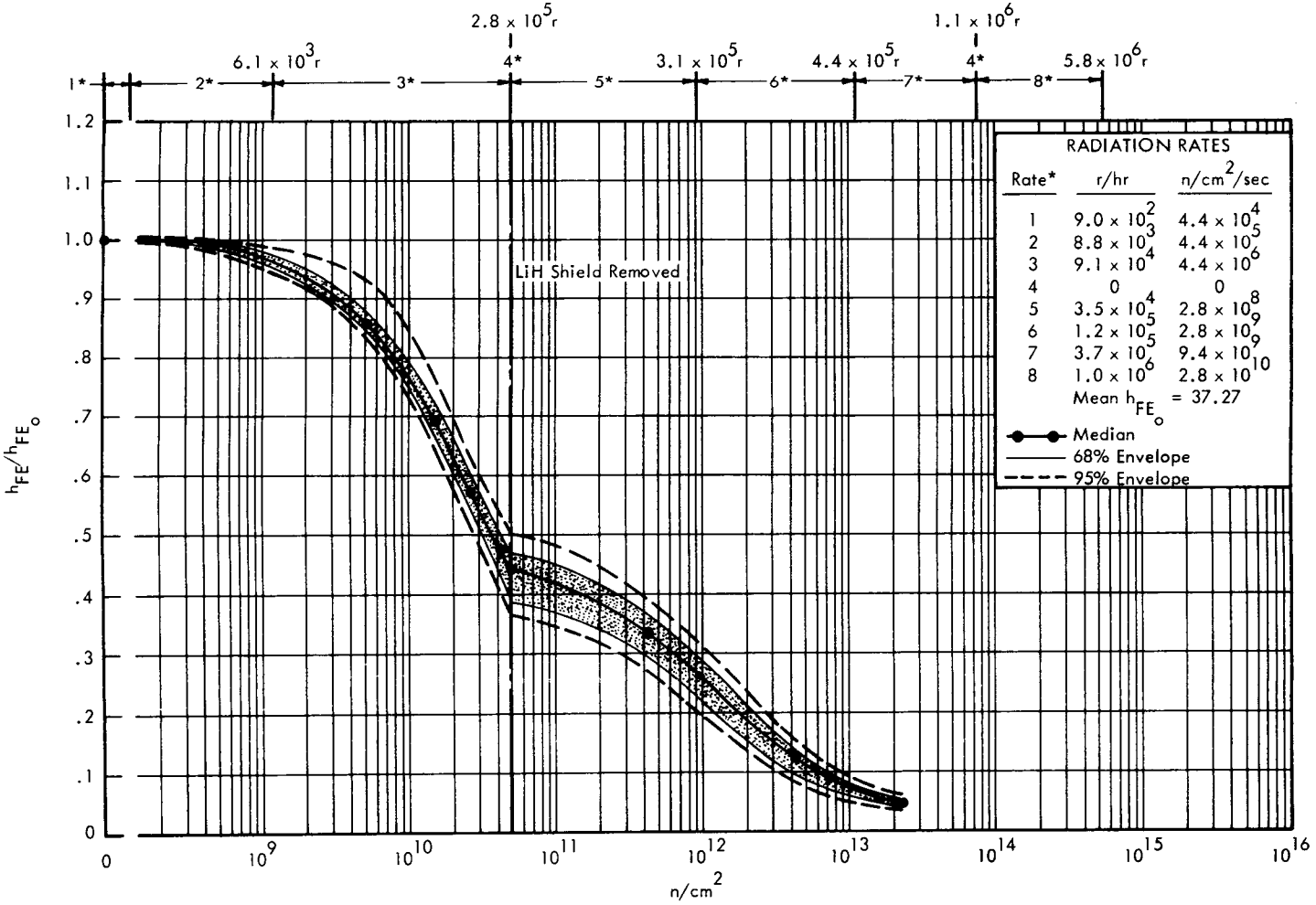

FIGURE 28 S2N1486 SILICON TRANSISTOR CORPORATION, 30°C, NORMALIZED h_{FE} VERSUS INTEGRATED NEUTRON FLUX

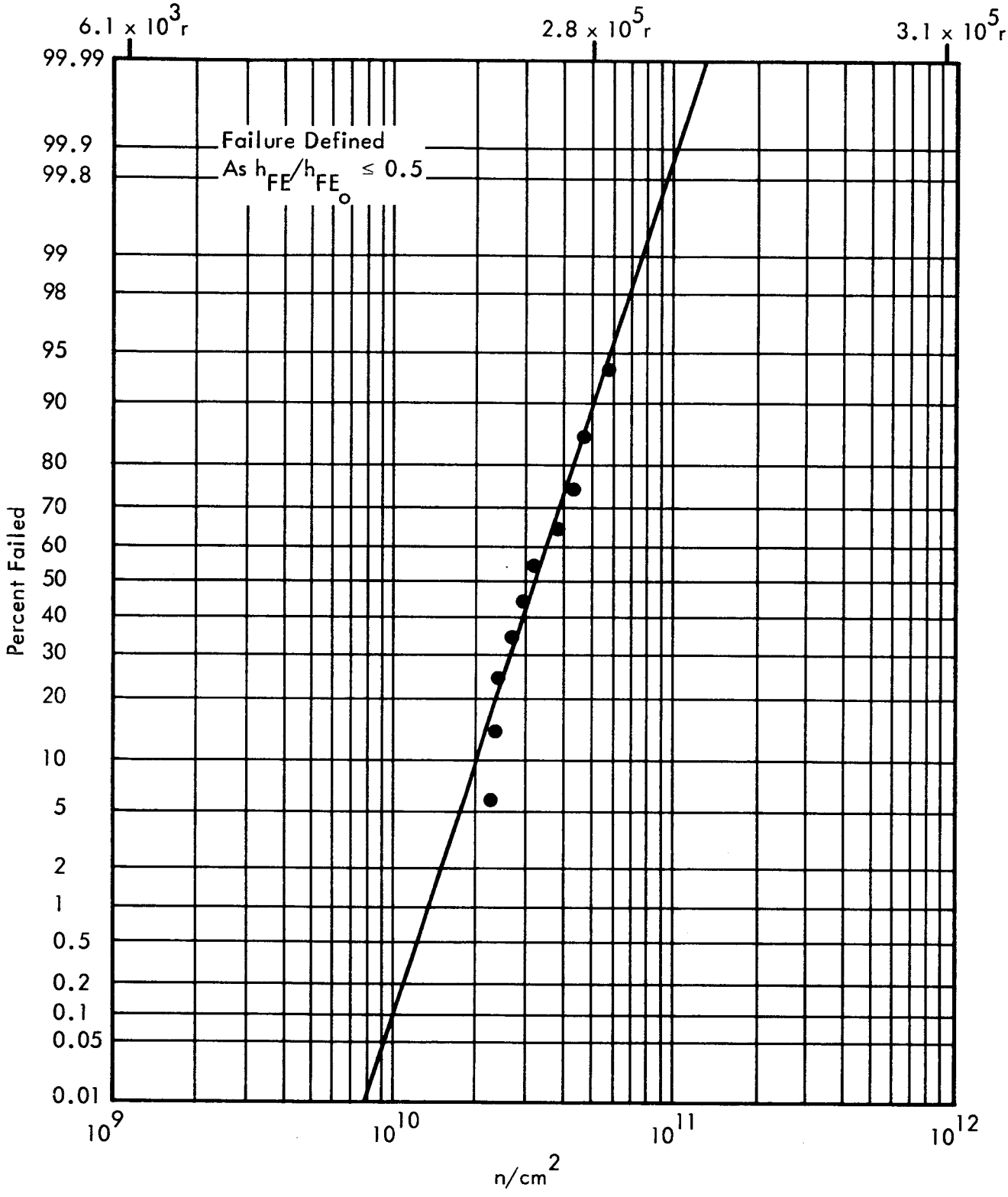

FIGURE 29 S2N1486 SILICON TRANSISTOR CORPORATION, 30°C, PERCENT FAILED VERSUS INTEGRATED NEUTRON FLUX

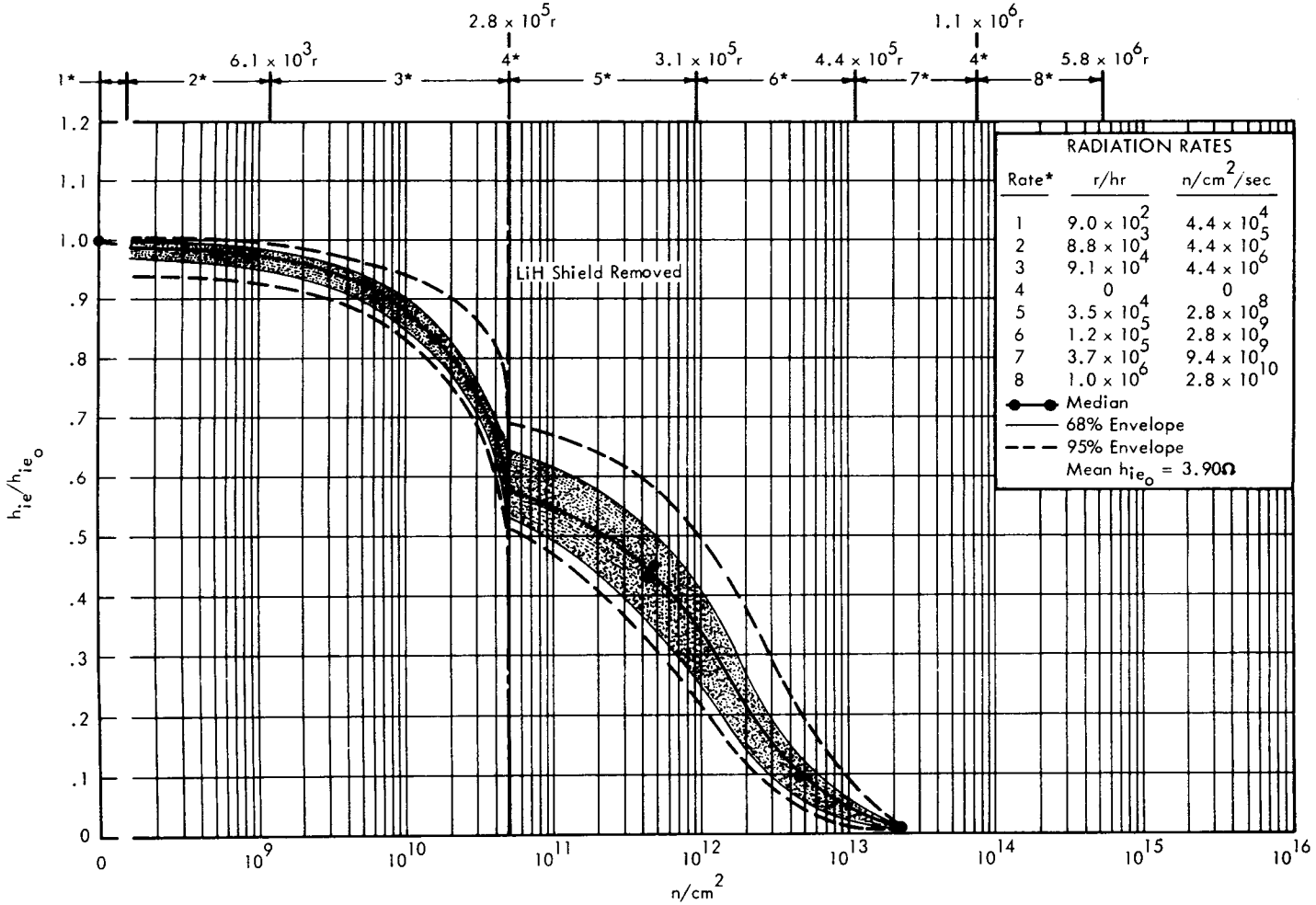

FIGURE 30 S2N1486 SILICON TRANSISTOR CORPORATION, 30°C, NORMALIZED h_{ie} VERSUS INTEGRATED NEUTRON FLUX

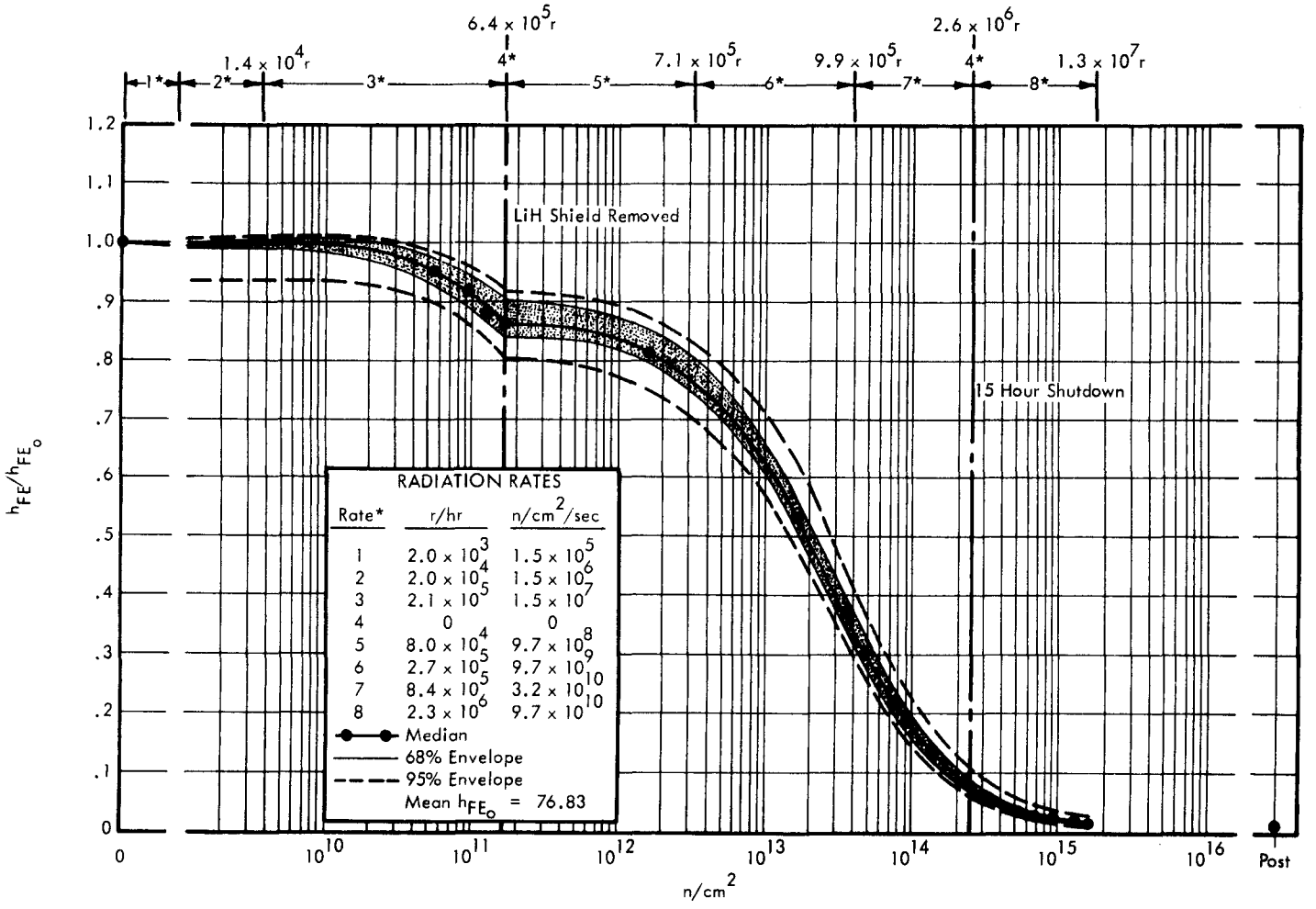

FIGURE 31 S2N2412 TEXAS INSTRUMENTS, 30°C, NORMALIZED h_{FE} VERSUS INTEGRATED NEUTRON FLUX

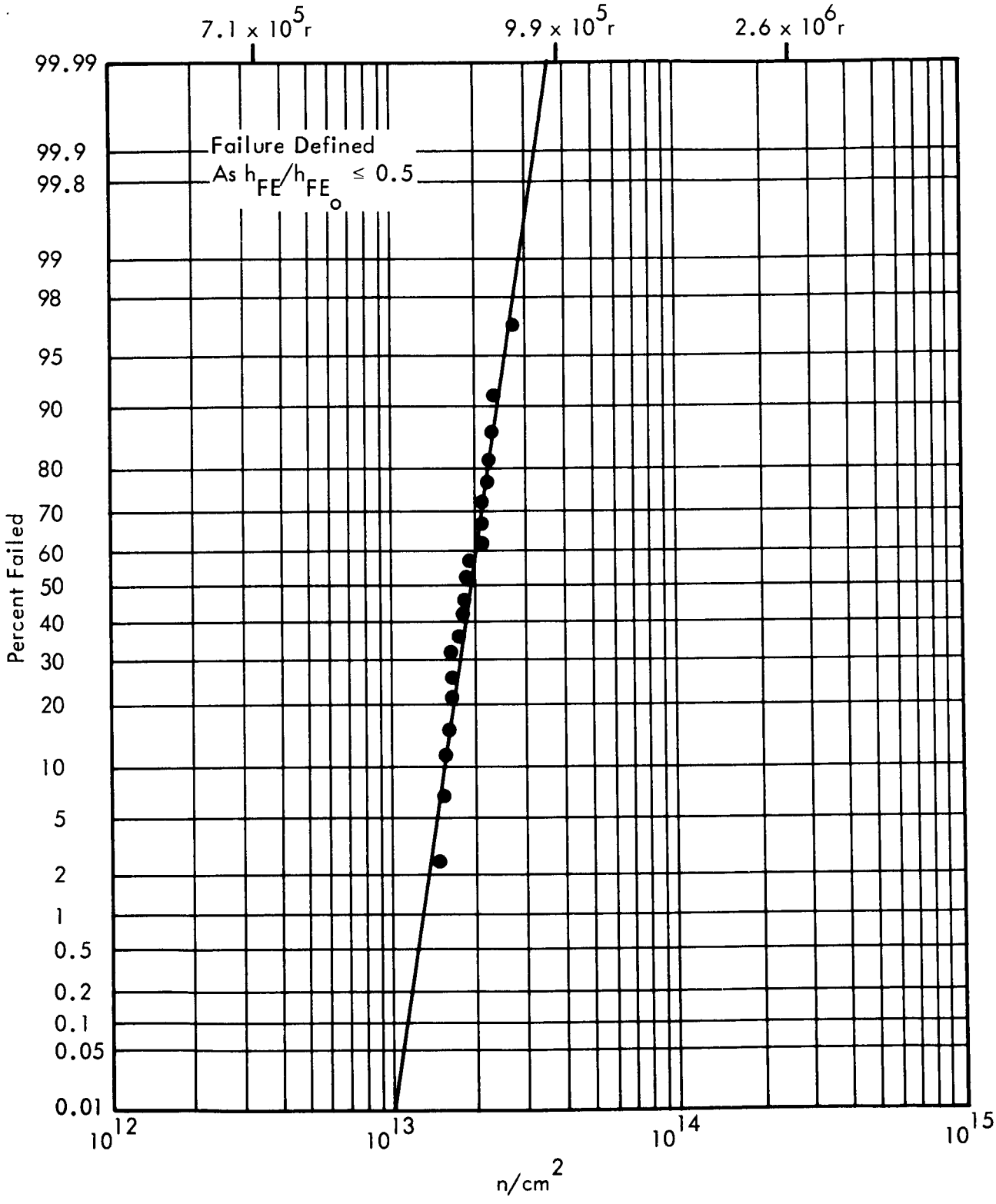

FIGURE 32 S2N2412 TEXAS INSTRUMENTS, 30°C, PERCENT FAILED VERSUS INTEGRATED NEUTRON FLUX

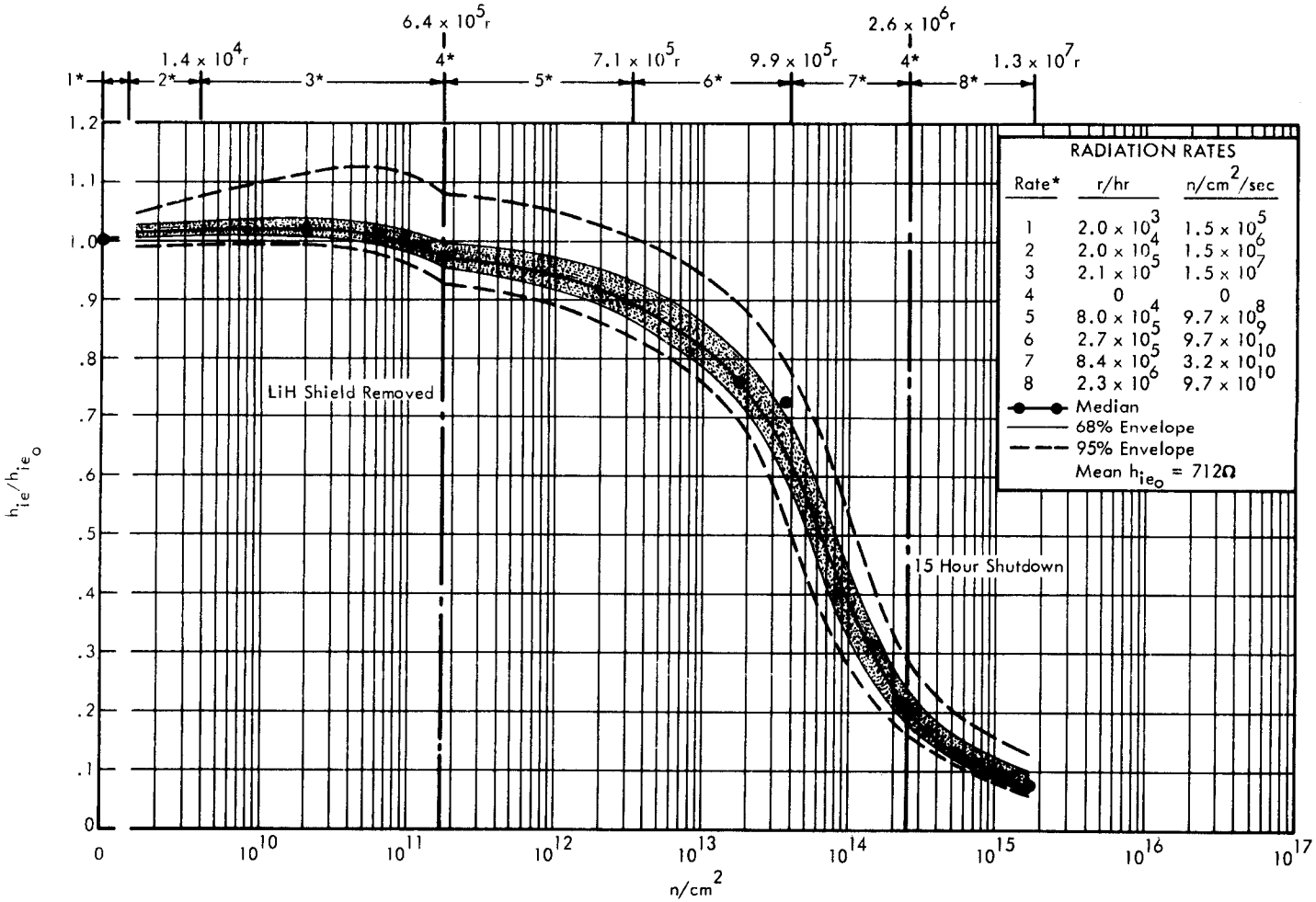

FIGURE 33 S2N2412 TEXAS INSTRUMENTS, 30°C, NORMALIZED h_{ie} VERSUS INTEGRATED NEUTRON FLUX

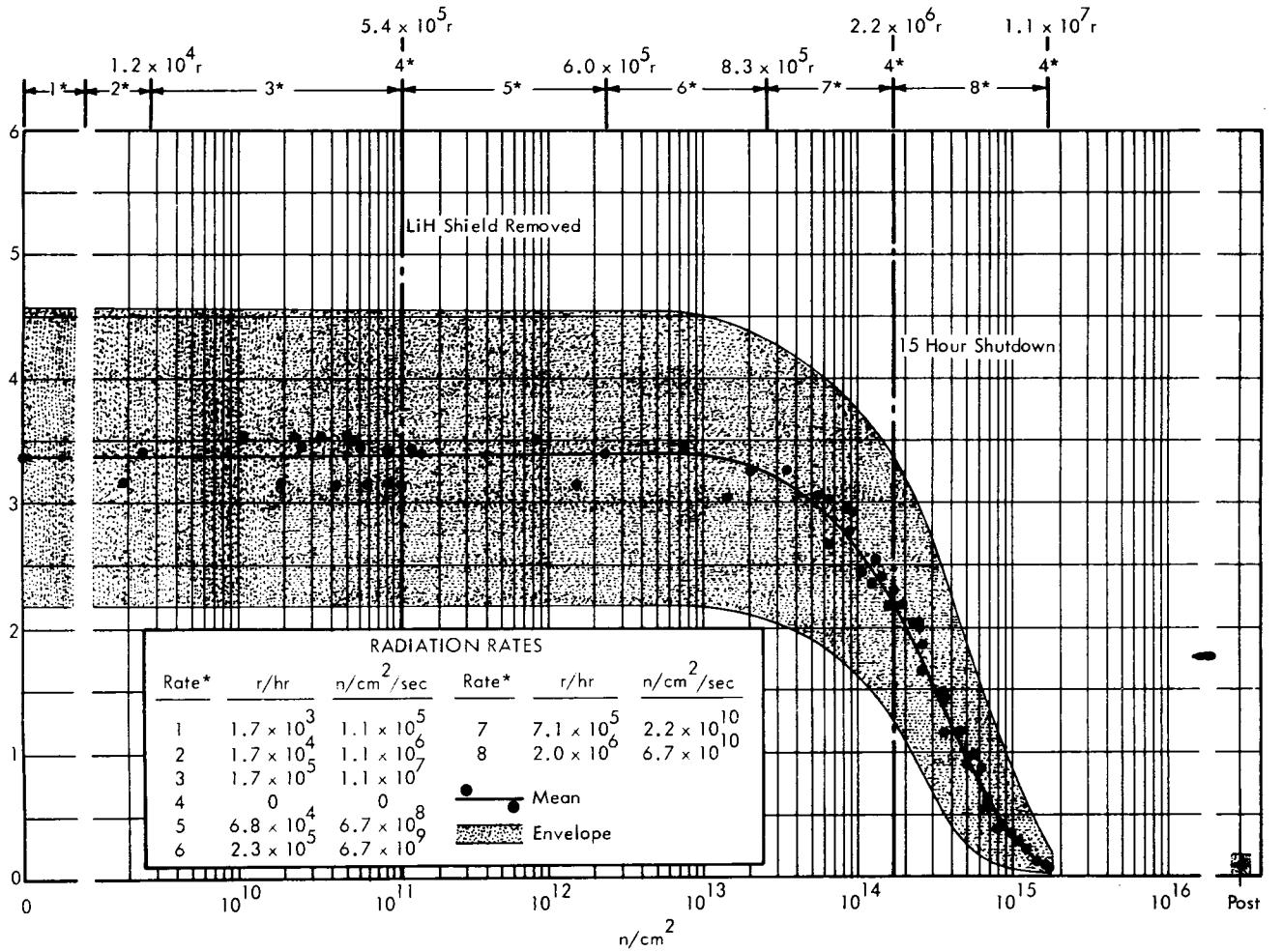

FIGURE 34 2N2498 TEXAS INSTRUMENTS, 30°C, I_{DSS} VERSUS INTEGRATED NEUTRON FLUX

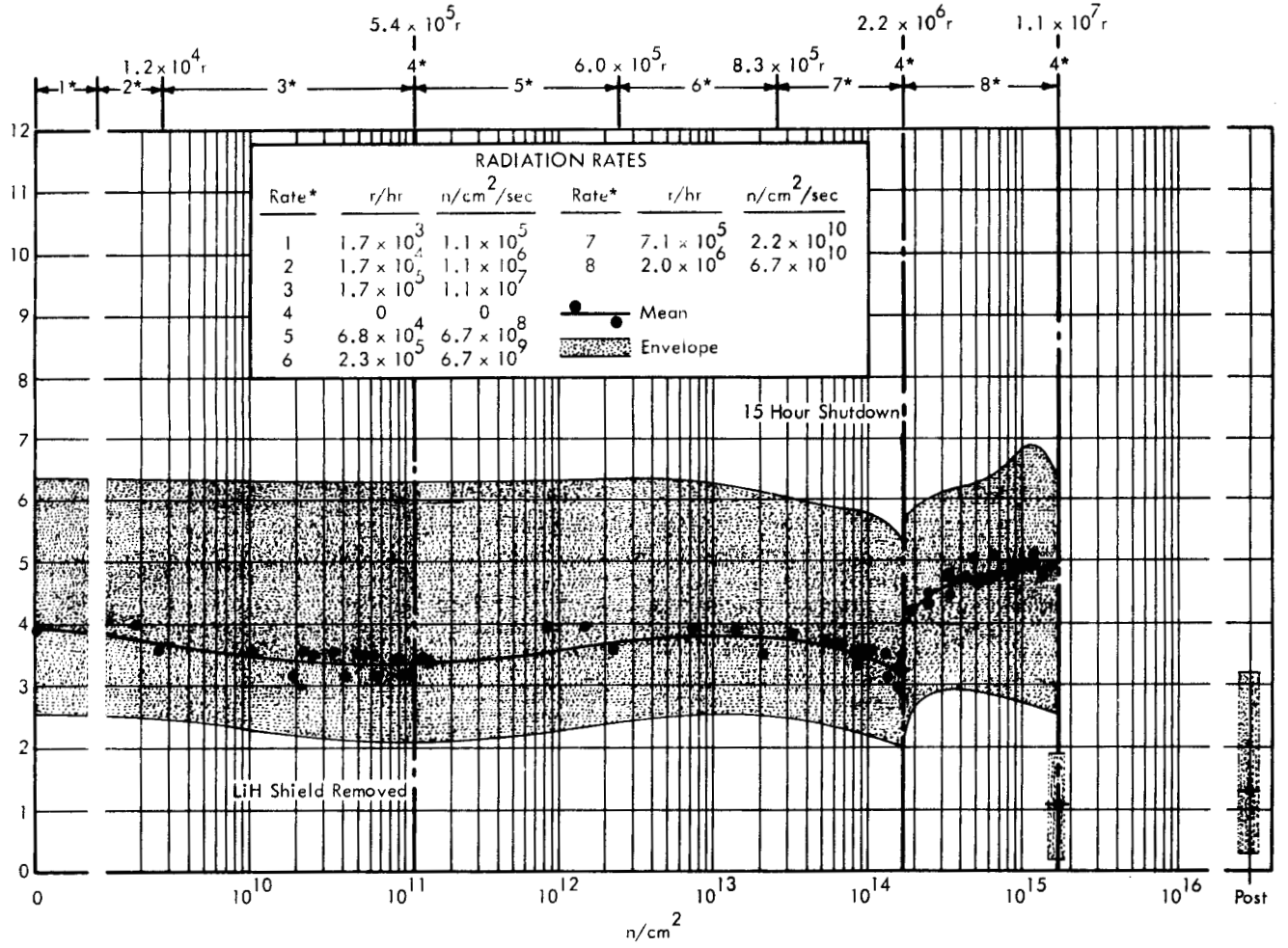

FIGURE 35 2N2498 TEXAS INSTRUMENTS, 30°C, V_p VERSUS INTEGRATED NEUTRON FLUX

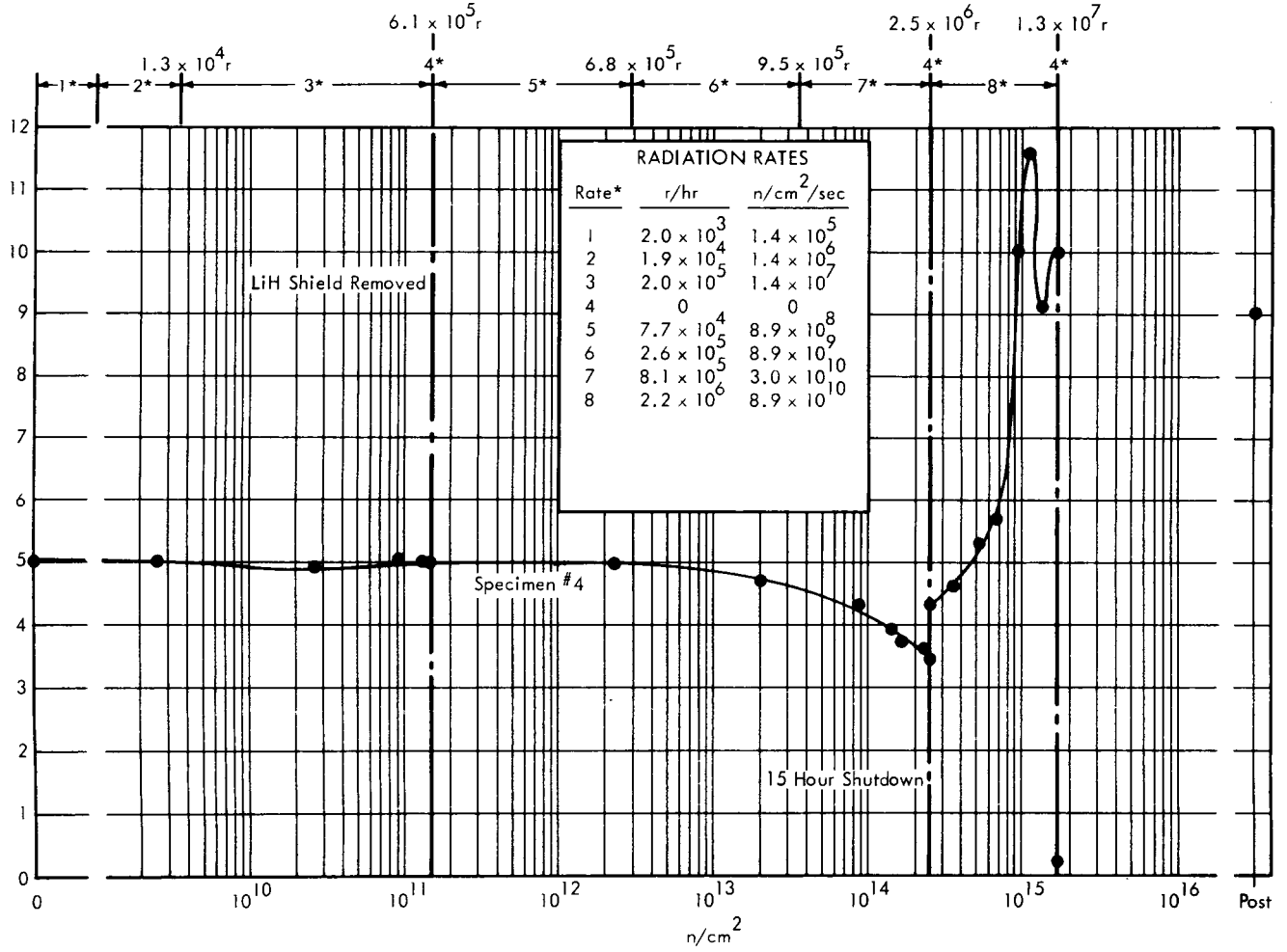

FIGURE 36 2N2498 TEXAS INSTRUMENTS, ONE UNUSUAL SPECIMEN, 30°C, V_P VERSUS INTEGRATED NEUTRON FLUX

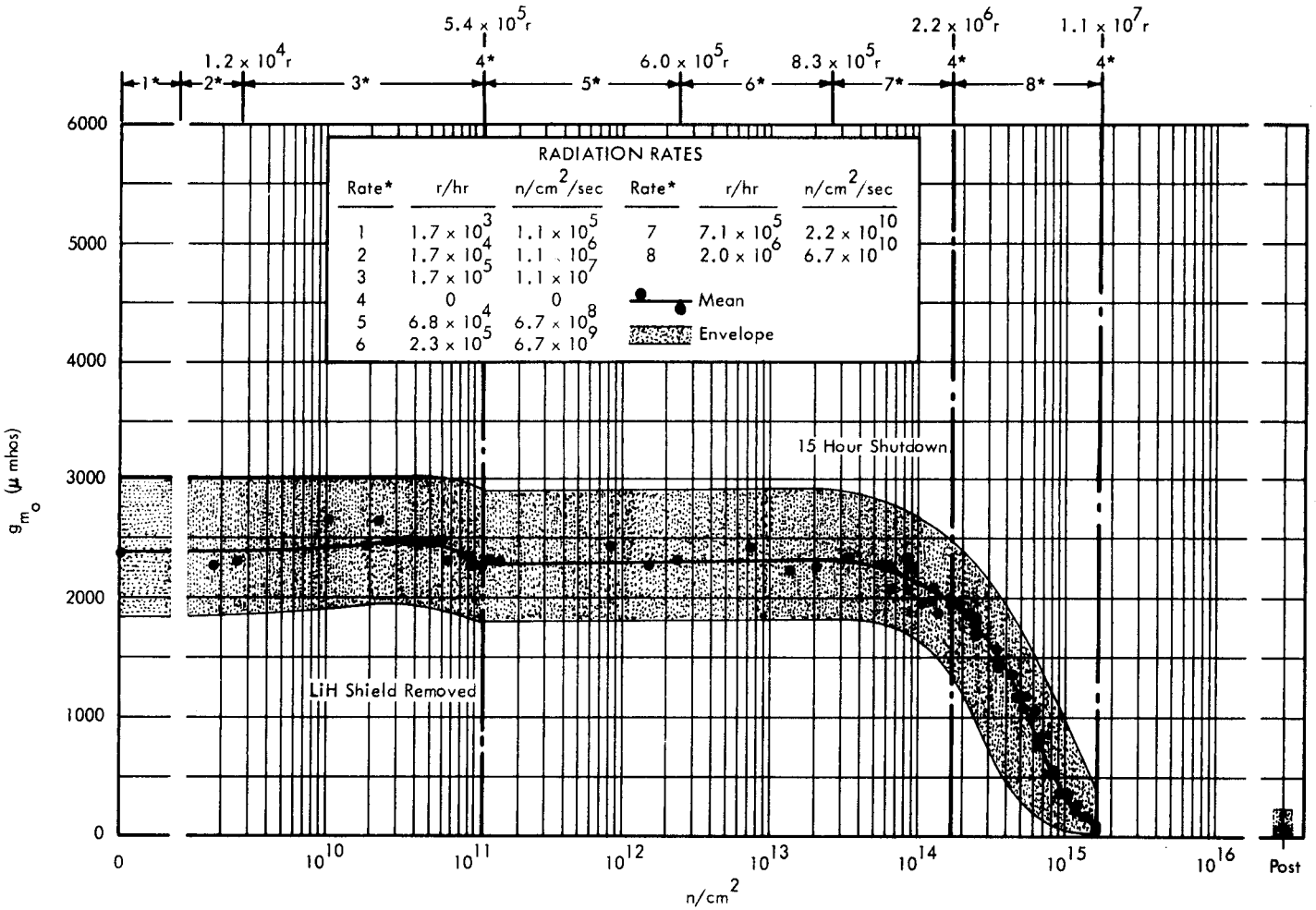

FIGURE 37 2N2498 TEXAS INSTRUMENTS, 30°C, g_{m_o} VERSUS INTEGRATED NEUTRON FLUX

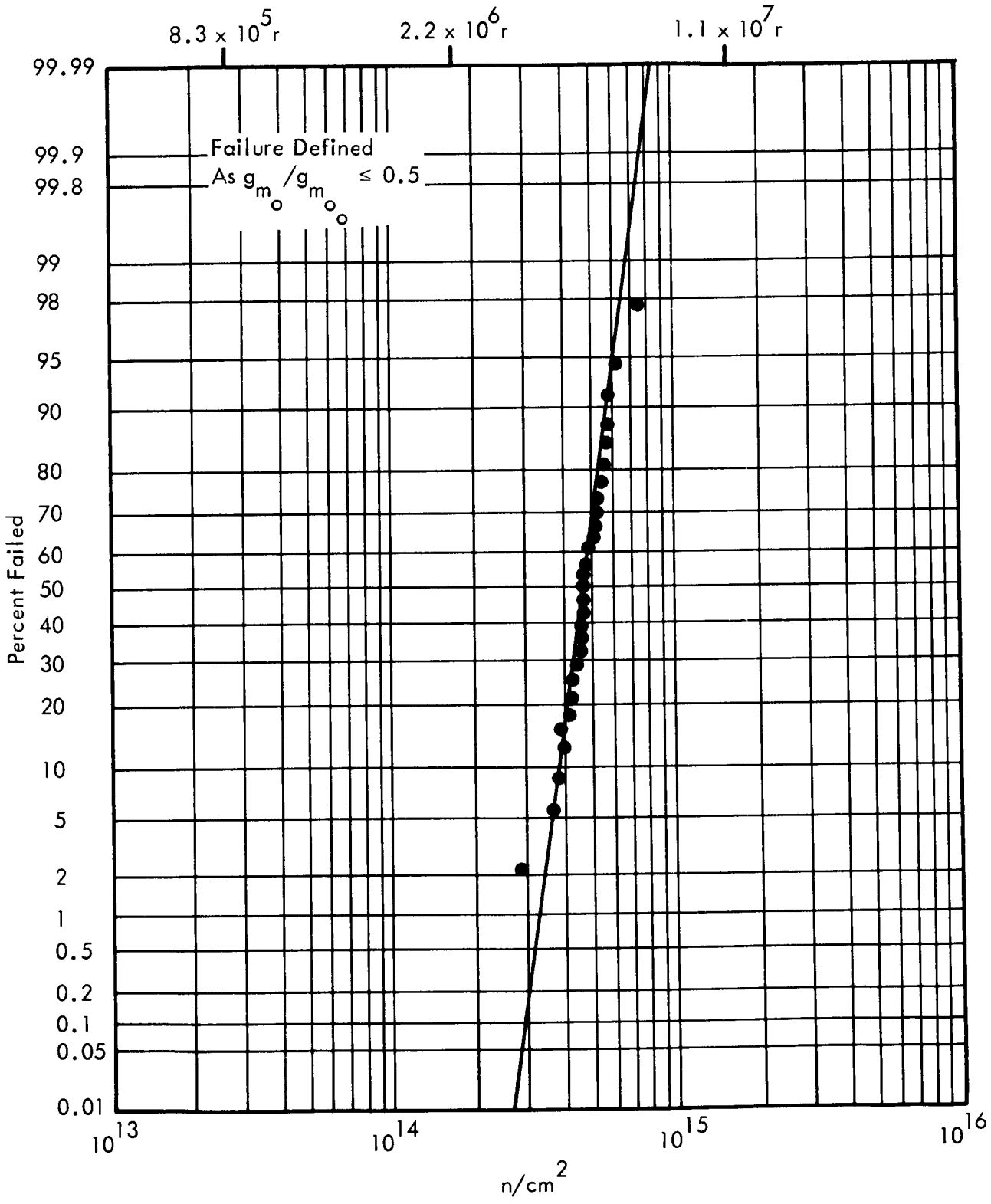

FIGURE 38 2N2498 TEXAS INSTRUMENTS, 30°C, PERCENT FAILED VERSUS INTEGRATED NEUTRON FLUX

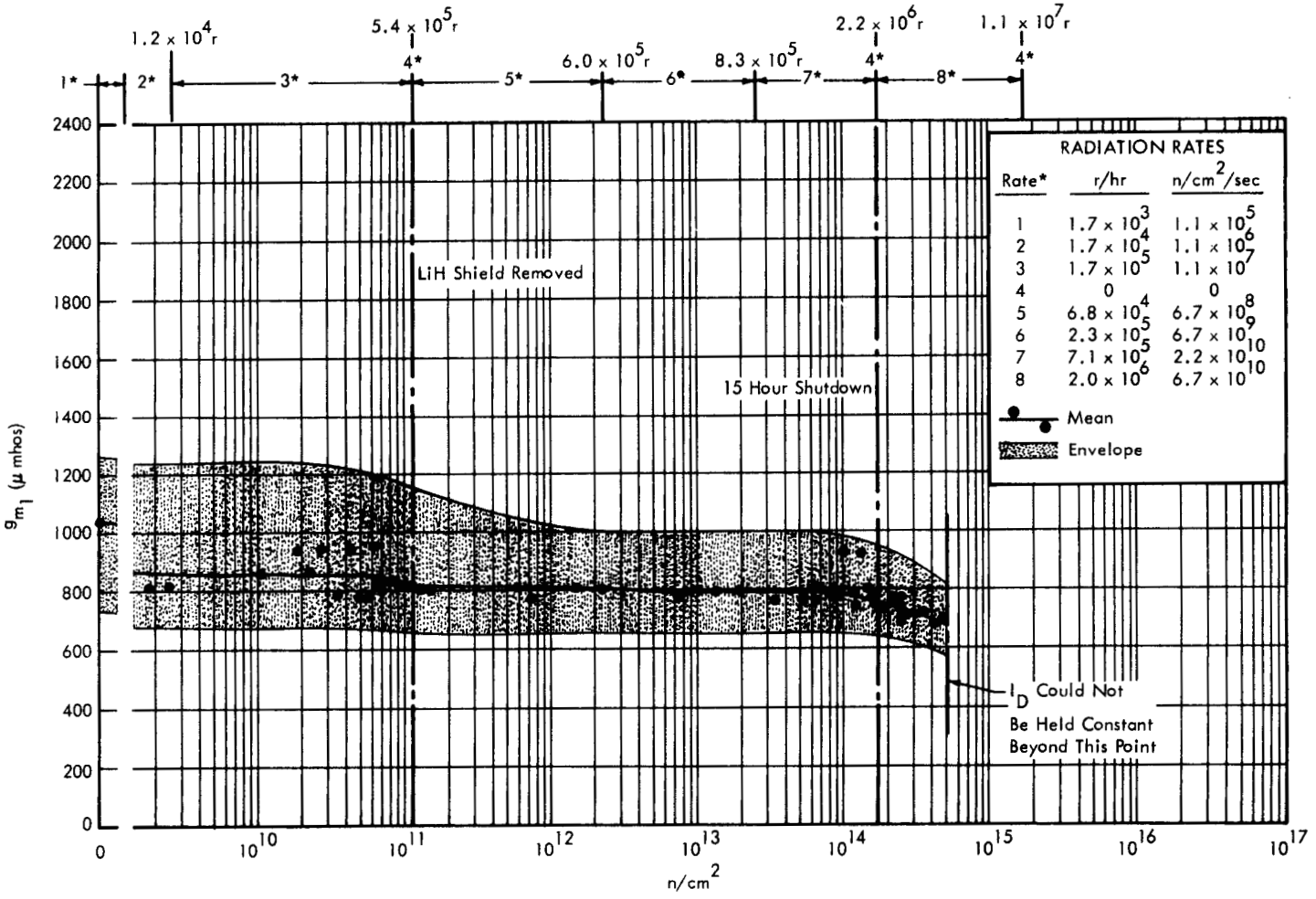

FIGURE 39 2N2498 TEXAS INSTRUMENTS, 30°C, g_{m_1} VERSUS INTEGRATED NEUTRON FLUX